

1 **Analogue experiments on releasing and restraining bends and their**  
2 **application to the study of the Barents Shear Margin**

3  
4  
5  
6 **Roy H. Gabrielsen<sup>1</sup>, Panagiotis A. Giannenas<sup>2</sup>, Dimitrios Sokoutis<sup>1,3</sup>, Ernst**  
7 **Willingshofer<sup>3</sup>, Muhammad Hassaan<sup>1,4</sup> & Jan Inge Faleide<sup>1</sup>**

8  
9 <sup>1</sup>Department of Geosciences, University of Oslo, Norway

10 <sup>2</sup>panagiotis-athanasios.giannenos@univ-rennes1.fr

11 <sup>3</sup>Faculty of Geosciences, Utrecht University, the Netherlands

12 <sup>4</sup>Vår Energi AS, Grundingen 3, 0250 Oslo, Norway

13  
14  
15 **Corresponding author: Roy H. Gabrielsen ([r.h.gabrielsen@geo.uio.no](mailto:r.h.gabrielsen@geo.uio.no))**

16  
17 **ORCI-id:**

18 Jan Inge Faleide: 0000-0001-8032-2015

19 Roy H. Gabrielsen: 0000-0001-5427-8404

20 Muhammad Hassaan: 0000-0001-6004-8557

21  
22  
23  
24  
25 **Abstract:**

26 The Barents Shear Margin separates the Svalbard and Barents Sea from the North  
27 Atlantic. During the break-up of the North Atlantic the plate tectonic configuration  
28 was characterized by sequential dextral shear, extension, and finally contraction  
29 and inversion. This generated a complex zone of deformation that contains several  
30 structural families of overlapping and reactivated structures. A series of crustal-  
31 scale analogue experiments, utilizing a scaled stratified sand-silicon polymer  
32 sequence were utilized in the study of the structural evolution of the shear margin.

33  
34 The most significant observations of particular significance for interpreting the  
35 structural configuration of the Barents Shear Margin are:

36 1) Prominent early-stage positive structural elements (e.g. folds, push-ups)  
37 interacted with younger (e.g. inversion) structures and contributed to a hybrid  
38 final structural pattern.

39 2) Several of the structural features that were initiated during the early (dextral  
40 shear) stage became overprinted and obliterated in the subsequent stages.

41 3) All master faults, pull-part basins and extensional shear duplexes initiated  
42 during the shear stage quickly became linked in the extension stage, generating a  
43 connected basin system along the entire shear margin at the stage of maximum  
44 extension.

45 4) The fold pattern generated during the terminal stage (contraction/inversion  
46 became dominant in the basin areas and was characterized by fold axes with  
47 traces striking parallel to the basin margins. These folds, however, most strongly  
48 affected the shallow intra-basin layers.

49 The experiments reproduced the geometry and positions of the major basins and  
50 relations between structural elements (fault and fold systems) as observed along

51 and adjacent to the Barents Shear Margin. This supports the present structural  
52 model for the shear margin.

53

54

55 **Plain language summary:**

56 The Barents Shear Margin defines the border between the relatively shallow  
57 Barents Sea that is situated on a continental plate, and the deep ocean. The margin  
58 is characterized by a complex structural pattern that has resulted from the  
59 opening and separation of the continent and the ocean, starting c. 55 million years  
60 ago. This history included one phase of right-lateral shear and one phase of  
61 oblique extension, the latter including a subphase of shortening, perhaps due to  
62 plate tectonic reorganizations. The area has been mapped by the study of  
63 reflection seismic lines for decades, but many details of its development is not yet  
64 fully constrained. We therefore ran a set of scaled experiments to investigate what  
65 kind of structures could be expected in this kind of tectonic environment, and to  
66 figure out what is a reasonable time relation between them. From these  
67 experiments we deduced several types of structures/faults, folds and  
68 sedimentary basins) that helps us to improve the understanding of the history of  
69 the opening of the North Atlantic.

70

71

72 **Key words:** Analogue experiments, dextral strike-slip, releasing and restraining  
73 bends, multiple folding, Barents Shear Margin, basin inversion

74

75

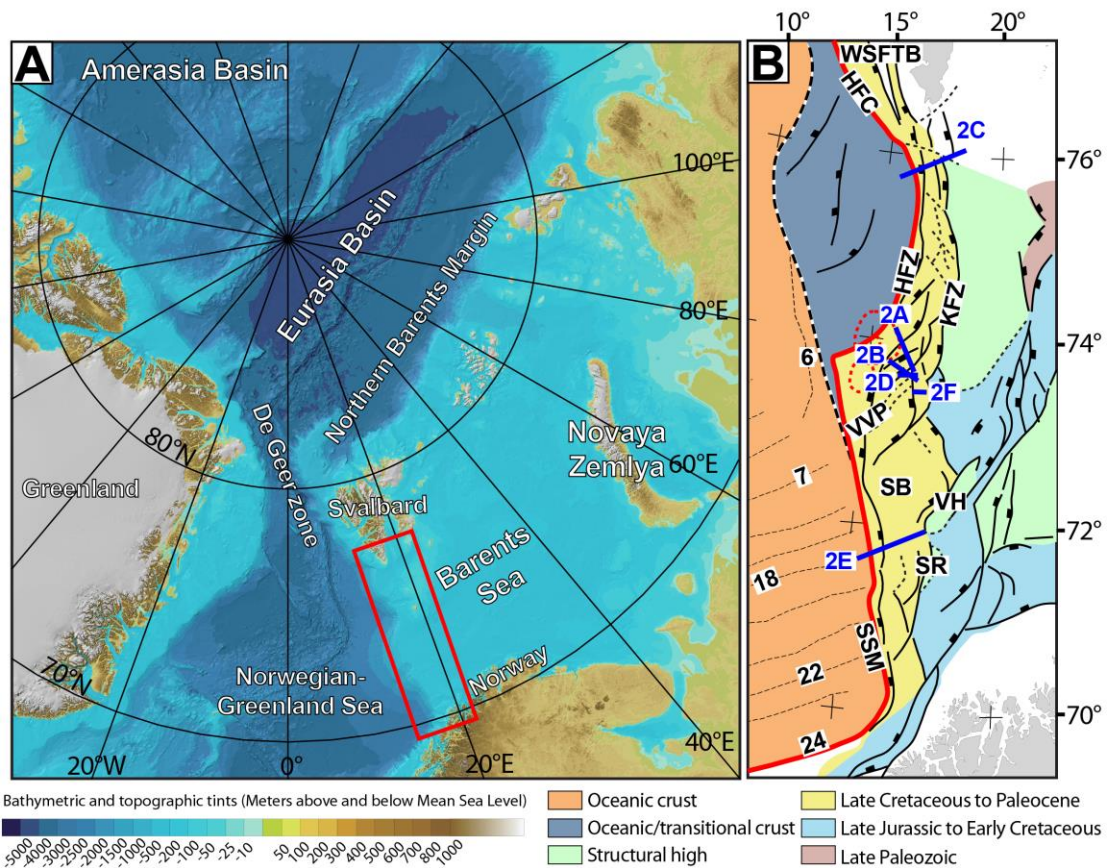
76 **Introduction**

77

78 Physiography, width and structural style of the Norwegian continental margin  
79 vary considerably along its strike (e.g. Faleide et al., 2008, 2015). The margin  
80 includes a southern rifted segment between 60° and 70°N and a northern sheared-  
81 rifted segment between 70° and 82°N (**Figure 1A**). The latter coincides with the  
82 ocean-ward border of the western Barents Sea and Svalbard margins (e.g. Faleide  
83 et al., 2008) and is referred to here as “the Barents Shear Margin”. This segment  
84 coincides with the continent-ocean transition (COT) of the northernmost part of  
85 the North Atlantic Ocean, and its configuration is typical for that of transform  
86 margins where the structural pattern became established in an early stage of  
87 shear, later to develop into an active continent-ocean passive margin (Masclé &  
88 Blarez, 1987; Lorenzo, 1997; Seiler et al., 2010; Basile, 2015; Nemcok et al., 2016).  
89 Palaeogene shear, rifting, breakup and incipient spreading in the North Atlantic  
90 was associated with voluminous magmatic activity, resulting in the development  
91 of the North Atlantic Volcanic Province (Saunders et al., 1997; Ganerød et al., 2010;  
92 Horni et al., 2017). According to its tectonic development, the Barents Shear  
93 Margin (**Figure 1B**) incorporates, or is bordered by, several distinct structural  
94 elements, some of which are associated with volcanism and halokinesis.

95

96 The multistage development combined with a complex geometry caused  
97 interference between structures (and sediment systems) in different stages of the  
98 margin development. Such relations are not always obvious, but interpretation  
99 can be supported by the help of scaled experiments. In combining the  
100 interpretation of reflection seismic data and analogue modeling, therefore, we  
101 investigate structures generated in (initial) dextral shear, the development into  
102 seafloor spreading and subsequent contraction in this process, the later stages of  
103 which were likely influenced by plate reorganization (Talwani & Eldholm, 1977;  
104 Gaina et al., 2009; see also Vågnes et al., 1998; Pascal & Gabrielsen, 2001; Pascal  
105 et al., 2005; Gac et al., 2016) and/or other far-field stresses (Doré & Lundin, 1996;  
106 Lundin & Doré, 1997; Doré et al., 1999; 2016; Lundin et al., 2013). The present  
107 experiments were designed to illuminate the structural complexity affiliated with  
108 multistage sheared passive margins, so that the significance of structural elements  
109 like fault and fold systems observed along the Barents Shear Margin could be set



110

111 **Figure 1: A)** The Barents Sea provides is separated from the Norwegian-  
 112 Greenland Sea by the De Geer Zone linking the North Atlantic to the Arctic Eurasia  
 113 Basin. Red box shows the present study area. **B)** Structural map Barents Sea shear  
 114 margin. Note segmentation of the continent-ocean transition. Abbreviations (from  
 115 north to south): WSFTB = West Spitsbergen Fold-and-Thrust Belt, HFZ =  
 116 Hornsund Fault Zone, KFZ = Knølegga Fault Zone, VVP = Vestbakken Volcanic  
 117 Province, SB = Sørvestsnaget Basin, VH = Veslemøy High, SR = Senja Ridge, SSM =  
 118 Senja Shear Margin. Blue lines indicate position of seismic profiles in Figure 2 and  
 119 red line in Figure 1B shows the western limitation of the thinned crust (see also  
 120 Figure 3). Chron numbers are indicated on oceanic crust area.

121

122 into a dynamic context. The study area suffered repeated and contrasting stages  
 123 of deformation, including dextral shear, oblique extension, inversion and volcanic  
 124 activity. This is a particular challenge in such tectonic settings, that are  
 125 characterized by repeated overprinting and cannibalization of incipient by  
 126 younger structural elements. The experimental approach opens for the  
 127 identification and characterisation of the different stages of deformation and their  
 128 affiliated structural elements on the way to the present-day margin geometry.

129

130

131 **Regional setting**

132 In the following sections we provide definitions and a short description of the  
133 most important structural elements constituting the study area. The structural  
134 elements are presented in-sequence from north to south (**Figure 1B**).

135

136 The greater **Barents Shear Margin** is a part of the preceding and more  
137 extensive “De Geer Zone megashear system which linked the Norwegian  
138 Greenland Sea and the Arctic Eurasia Basin system (Eldholm et al., 1987; 2002;  
139 Faleide et al., 1988; Breivik et al., 1998; 2003). Together with its conjugate  
140 Greenland counterpart it carries the evidence of an extensive period of structural  
141 development, starting with post-Caledonian (Devonian) extension and  
142 culminating with Palaeogene break-up of the North Atlantic (e.g., Brekke, 2000;  
143 Gabrielsen et al., 1990; Faleide et al., 1993; 2008; Gudlaugsson et al., 1998;  
144 Tsikalas et al., 2012). Two shear margin segments that are separated by a central  
145 rift-dominated segment can be identified in the Barents Shear Margin (Myhre et  
146 al., 1982; Vågnes, 1997; Myhre & Eldholm, 1988; Ryseth et al., 2003; Faleide et al.,  
147 1988; 1993; 2008). Each segment maintained a particular signature concerning  
148 the structural and magmatic characteristics of the crust during its development.  
149 Of these the Senja Shear Margin is the southernmost segment, originally termed  
150 the Senja Fracture Zone by Eldholm et al. (1987). Here, NNW-SSE-striking folds  
151 interfere with folds with NE-SW-striking axes. Strain partitioning may also have  
152 affected some of the other shear zone segments of the study area (Sørvestsnaget  
153 Basin; Kristensen et al., 2017). Shearing contributed to the development of  
154 releasing and restraining bends, associated pull-apart-basins, neutral strike-slip  
155 segments, flower-structures and fold-systems (*sensu* Crowell, 1974 a,b; Biddle &  
156 Christie-Blick, 1985a,b; Cunningham & Mann, 2007a,b). Particularly the hanging  
157 wall west of the Knølegga Fault Complex (see below) of the Barents Shear Margin  
158 was affected by wrench deformation as seen from several push-ups and fold  
159 systems (Grogan et al., 1999; Bergh & Grogan 2003).

160

161 **The Hornsund Fault Zone and West Spitsbergen Fold-and Thrust Belt** form  
162 the northernmost segment of the Barents Shear Margin and coincide with the  
163 northern continuation of the De Geer Zone. The presently distinguishable master

164 fault of this system is the Hornsund Fault Zone, which together with the West  
165 Spitsbergen fold-and-thrust-belt provides a type setting for transpression and  
166 strain partitioning (Harland, 1965; 1969; 1971; Lowell, 1972; Gabrielsen et al.,  
167 1992; Maher et al., 1997; Leever et al., 2011 a,b). Plate tectonic reconstructions  
168 suggest that the plate boundary accommodated c. 750 km along-strike  
169 displacement and 20-40 km of shortening in the Eocene (Bergh et al., 1997; Gaina  
170 et al., 2009).

171

172 **The Knølegga Fault Zone** can be seen as a part of the Hornsund fault system  
173 extending from the southern tip of Spitsbergen (Gabrielsen et al., 1990). It trends  
174 NNE-SSW to N-S and defines the western margin of the Stappen High. The vertical  
175 displacement approaches 6 km, being the cumulative effect of several phases of  
176 faulting throughout Late Paleozoic, Mesozoic and Cenozoic times. The Cenozoic  
177 displacement may have had a lateral (dextral) component (Gabrielsen et al.,  
178 1990).

179

180 **The Vestbakken Volcanic Province** is the central topic of the present  
181 contribution. It represents the rifted segment of the Barents Shear Margin and  
182 links the sheared margin segments that are situated to the north and south of it  
183 and occupies a typical right-double (eastward) stepping releasing-bend-setting.  
184 Prominent volcanoes and sill-intrusions display significant magmatic activity, and  
185 three distinct volcanic events are distinguished in the Vestbakken Volcanic  
186 Province (Jebsen & Faleide, 1998; Faleide et al., 2008; Libak et al., 2012). The area  
187 has been affected by complex tectonics and both extensional and contractional  
188 structures are observed. The Vestbakken Volcanic Province is delineated towards  
189 the east by an extensional top-west fault zone that parallels the Knølegga Fault  
190 Complex). The interior of the Vestbakken Volcanic Province is dominated by NE-  
191 SW-striking extensional faults and associated fault blocks. Positive structural  
192 elements include inverted fault blocks, and wide-angle ( $\lambda > 20$  km) anticlines (roll-  
193 over anticlines?) and domes that are overprinted by faults and folds with  
194 amplitudes and wavelengths on the hundred- and km-scales.

195

196 The Eastern Boundary Fault (EBF) is a top-west normal fault with a regional NNE-  
197 SSW strike, consisting of two separate, linked segments. Its northern segment  
198 dips more steeply to the WNW than the southern segment. The total vertical  
199 displacement as measured on the early Eocene level is in the order of 300 ms (450  
200 m), and the upper part of the hanging wall displays a normal drag modified by  
201 hanging wall tight anticline suggesting post-early Miocene inversion. Several  
202 normal, dominantly NE-SW-striking NW-facing normal faults transect the hanging  
203 wall of the EBF-fault. The Central Fault (CF) is the most prominent of those and is  
204 hard-linked to the central segment of the EBF-fault. All other faults in this map are  
205 secondary faults, mainly acting as accommodation structures to the master faults.  
206 Starting from the southern part of the area and south of the well site, a population  
207 of secondary faults is expressed as anastomosing faults traces.

208

209 Two main episodes of Cenozoic extensional faulting were identified in the  
210 Vestbakken Volcanic Province: (i) a late Paleocene-early Eocene event, which  
211 correlates in time with continental break-up in the Norwegian-Greenland Sea, and  
212 (ii) an early Oligocene event is tentatively correlated to plate reorganization  
213 around 34 Ma activating mainly NE-SW striking faults. Evidence of volcanic  
214 activity coincide with both of these events. Additional extensional events are  
215 recorded in mid-Eocene, late Oligocene and early Miocene times (Jebsen, 1998).  
216 The Vestbakken Volcanic Province is constrained to its east by the eastern  
217 boundary fault (EBF in **Figure 1B**), that is a part of the Knølegga Fault Zone,  
218 separating the Vestbakken Volcanic Province from the marginal Stappen High  
219 further to the east (Blaich et al., 2017). To the south and southeast the Vestbakken  
220 Volcanic Province drops gradually into the Sørvestsnaget Basin across the  
221 southern extension of the eastern boundary fault and its associated faults. To the  
222 west and north the area is delineated by the continent–ocean  
223 boundary/transition.

224

225 **The Sørvestsnaget Basin** occupies the area east of the COT between 71 and 73°N  
226 and is characterized by an exceptionally thick Cretaceous-Cenozoic sequence  
227 (Gabrielsen et al., 1990). To the west it is delineated by the Senja Shear Margin  
228 and to the northeast it is separated from the Bjørnøya Basin by the southern part

229 of the Knølegga Fault Complex (Faleide et al., 1988). The position of the Senja  
230 Ridge coincides with southeastern border of the Sørvestsnaget Basin (Figure 1B),  
231 whereas the Vestbakken Volcanic Province is situated to its north. An episode of  
232 Cretaceous rifting in the Sørvestsnaget Basin seems to have climaxed in the  
233 Cenomanian-middle Turonian (Breivik et al., 1998) to become succeeded by Late  
234 Cretaceous-Palaeocene fast sedimentation (Ryseth et al., 2003). Particularly the  
235 later stages of the basin development were strongly influenced by the opening of  
236 the North Atlantic (Hanisch, 1984; Brekke & Riis, 1987). Salt diapirism did also  
237 contribute to structuring of this basin (Perez-Garcia et al., 2013).

238

239 **The Senja Ridge** runs parallel to the continental margin and coincides with the  
240 western border of the Tromsø Basin. It is characterized by a N-S-trending gravity  
241 anomaly which are interpreted as buried mafic-ultramafic intrusions which are  
242 associated with the Seiland Igneous Province (Fichler & Pastore, 2022). The  
243 structural development of the Senja Ridge has been associated with shear  
244 affiliated with the development of the shear margin (Riis et al., 1986).

245

246 **The Senja Shear Margin** was active during the Eocene opening of the Norwegian-  
247 Greenland Sea during dextral shear that was accompanied by splitting out slivers  
248 of continental crust that became isolated units embedded by oceanic crust during  
249 seafloor spreading (Faleide et al., 2008). The Senja Shear Margin coincides with  
250 the western margin of a basin system that is characterized by significant crustal  
251 thinning and sedimentary thicknesses of 18-20 km. This part of the shear margin  
252 was characterized by a composite architecture even at the earliest stages of its  
253 development (Faleide et al., 2008). The structural development of the Senja Shear  
254 Margin was complicated by active halokinesis in the Sørvestsnaget Basin (Knutsen  
255 & Larsen, 1997; Gudlaugsson et al., 1998; Ryseth et al., 2003).

256

## 257 **Data and structural interpretation**

258

259 The data set of this study includes 2D seismic reflection data from several surveys  
260 and well data in the Vestbakken Volcanic Province. Data coverage is less dense in  
261 northern part of the study area. Typical spacing of seismic lines is 4 km. Well



262 7316/5-1 was used to correlate the seismic data with formation tops in the study  
263 area whereas published paper based correlations provided calibration and age of  
264 each seismic horizon mapped (e.g. Eidvin et al., 1993; 1998; Ryseth et al., 2003).  
265 Three stratigraphic groups are present in the well; the Nordland Group (473 - 945  
266 m); the Sotbakken Group (945-3752m) and Nygrunnen Group (3752-4014m)  
267 (Eidvin et al., 1993; 1998; [www.npd.com](http://www.npd.com)).

268

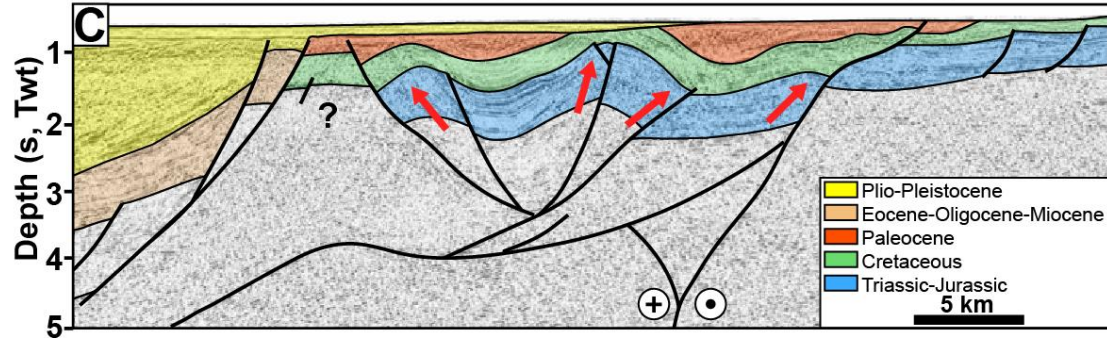
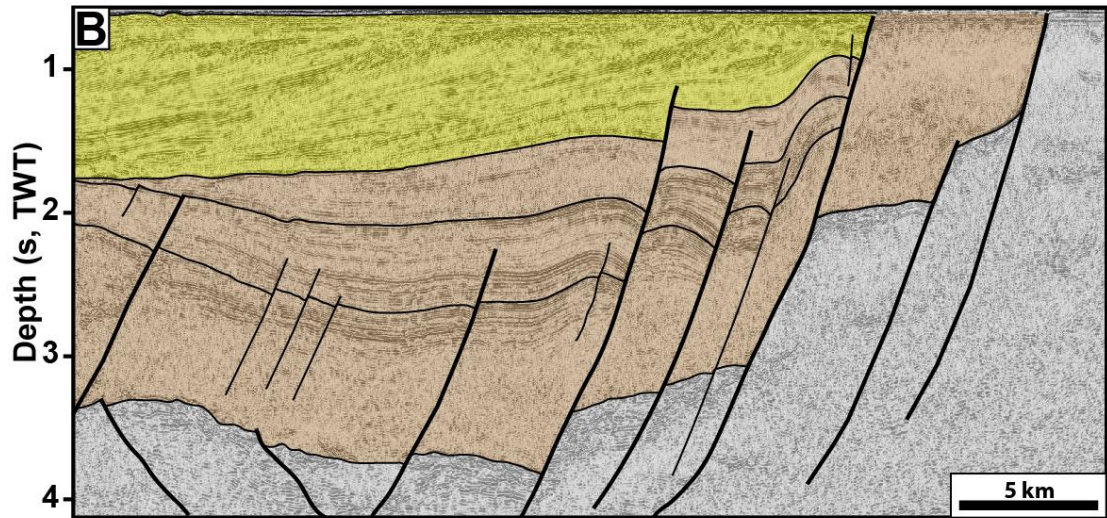
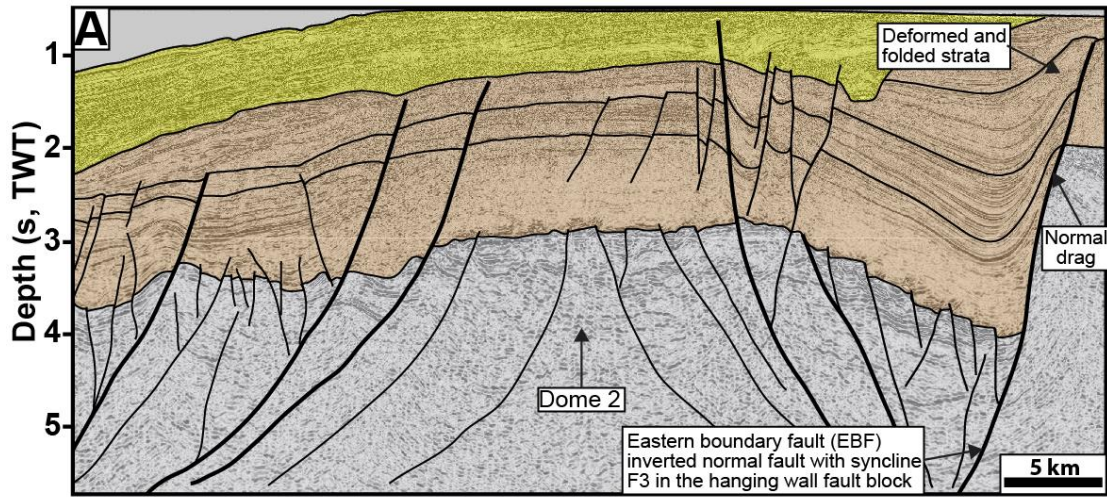
269 Several folds of regional significance and with axial traces that can be followed  
270 along strike for 2-3 km or more occur in the Vestbakken Volcanic Province. The  
271 folds commonly are situated in the hanging walls of extensional faults and the fold  
272 traces and the structural grain of the thick-skinned master faults are generally  
273 parallel. This shows that the position and orientation of the folds were determined  
274 by the preexisting structural fabric affiliated with these faults. The continuity of  
275 the folds remains obscure due to spacing of reflection seismic lines, so each fold  
276 may include undetected overlap zones or axial off-sets that have not been  
277 detected. The folds were identified on the lower Eocene, Oligocene and lower  
278 Miocene levels. All the mapped folds are either positioned in the hanging walls of  
279 extensional (sometimes inverted) master faults or are dissected by younger faults  
280 with minor throws.

281

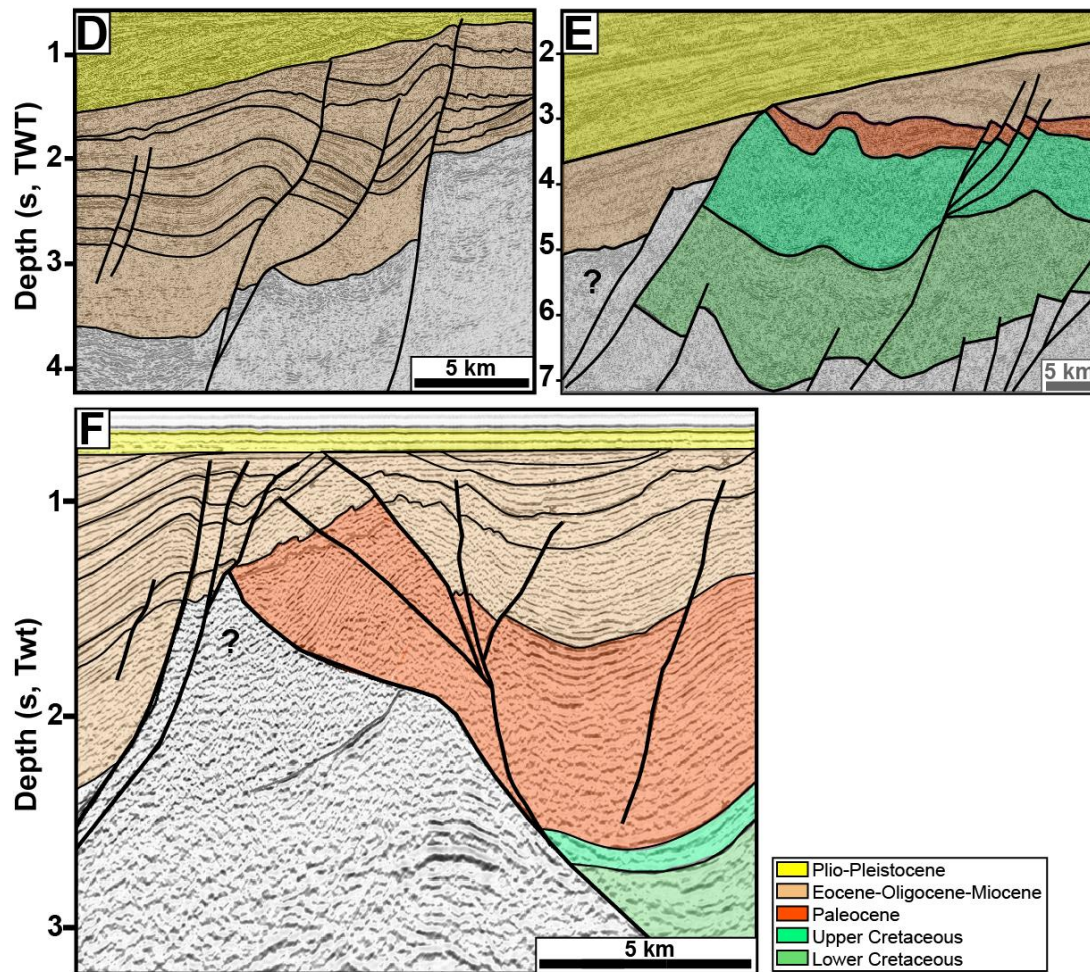
## 282 **Strike-slip systems and analogue shear experiments**

283

284 Shear margins and strike-slip systems are structurally complex and highly  
285 dynamic, so that the eventual architecture of such systems include structural  
286 elements that were not contemporaneous (e.g., Graymer et al., 2007; Crowell,  
287 1962; 1974a,b; Woodcock & Fischer, 1986; Mousloupoulou et al., 2007; 2008).  
288 Analogue models offer the option to study the dynamics of such relations and  
289 therefore attracted the attention of early workers in this field (e.g., Cloos 1928;  
290 Riedel 1929) and have continued to do so until today. Early experimental works  
291 mostly utilized one-layer ("Riedel-box") models (e.g. Emmons 1969; Tchalenko,  
292 1970; Wilcox et al., 1973), which were soon to be expanded by the study of  
293 multilayer systems (e.g. Faugère et al., 1986; Naylor et al., 1986; Richard et al.,







295

296 **Figure 2:** Seismic examples from various segments of the Barents Sea shear  
 297 margin. **A)** Gentle, partly collapsed NE-SW-striking anticline/dome in the eastern  
 298 terrace domain of the southern Vestbakken Volcanic Province. The origin of this  
 299 structure is obscure, but one can speculate that some of the open syncline-  
 300 anticline pairs originated as PSE-1-structures. **B)** Flower (PSE-2)-structure in area  
 301 dominated by neutral shear. **C)** Section through push-up (PSE-4-structure)  
 302 associated with restraining bend. **D-E)** Asymmetrical folds situated along the  
 303 eastern margin of the Vestbakken Volcanic Province, representing primary PSE-  
 304 5-structures. These structures are focused in the hangingwalls along the  
 305 escarpments of master fault blocks. **F)** Trains of symmetrical folds with upright  
 306 fold axes (PSE-6-structure family) are preserved inside larger fault blocks. See  
 307 Table 1 and text for explanation of the PSE-structures.  
 308

309 1991; Richard & Cobbold, 1989, 1995; Schreurs, 1994, 2003; Manduit & Dauteuil,  
 310 1996; Dateuil & Mart, 1998; Schreurs & Colletta, 1998, 2003; Ueta et al., 2000;  
 311 Dooley & Schreurs, 2012). The systematics and dynamics of strike-slip systems  
 312 have been focused upon in a number of summaries like Sylvester (1985; 1988);  
 313 Biddle & Christie-Blick (1985a,b); Cunningham & Mann (2007); Dooley &  
 314 Schreurs (2012); Nemcok et al. (2016) and Peacock et al. (2016). Concepts and

315 **Table 1**  
 316 Characteristics of Positive Structural Elements (PSE-1 -PSE-6) as described in text and shown in figures. Note that PSE-1-structures that  
 317 were developed in the earliest stages of the experiments became cannibalized or obliterated during the continued deformation. No  
 318 candidates of this structure population were identified with certainty in reflection seismic sections.  
 319

<b>Struct. type</b>	<b>Structural configuration</b>	<b>Orientation</b>	<b>Expr. stage</b>	<b>Segment</b>	<b>Recognized in seismic</b>	<b>Figure Expr</b>	<b>Figure Seism</b>
<b>PSE-1</b>	Open syn-anticline system	135 deg	Stage 1	1,3	?	5,6	1A?
<b>PSE-2</b>	Incipient flower or half-flower	Parallel master fault	Stage 1	1,2,3	Yes	5,6,8	1B
<b>PSE-3</b>	Forced folds above rotated fault blocks	Parallel master fault in releasing bend	Stage 2	1,2	Yes	9B	
<b>PSE-4</b>	Push-up	Parallel master fault in restraining bend	Stage 1	2	Yes	9D	1C
<b>PSE-5</b>	Anticlines/snake-heads in hanging walls	Parallel master faults	Stage 3	1,2,3	Yes	9C,D	1D,E
<b>PSE-6</b>	Anticline-syncline trains	Parallel master faults	Stage 3	1,2,3	Yes	12	1F

320

321 nomenclature established in these works are used in the following descriptions  
322 and analysis. Also, following Christie-Blick & Biddle (1985a,b) and Dooley &  
323 Schreurs (2012) we apply the term Principal Deformation Zone (PDZ) for the  
324 junction between the movable polythene plates underlying the experiment. The  
325 contact between the fixed and movable base defined a non-stationary velocity  
326 discontinuity (“VD”; Ballard et al., 1987; Allemand & Brun, 1991; Tron & Brun,  
327 1991).

328

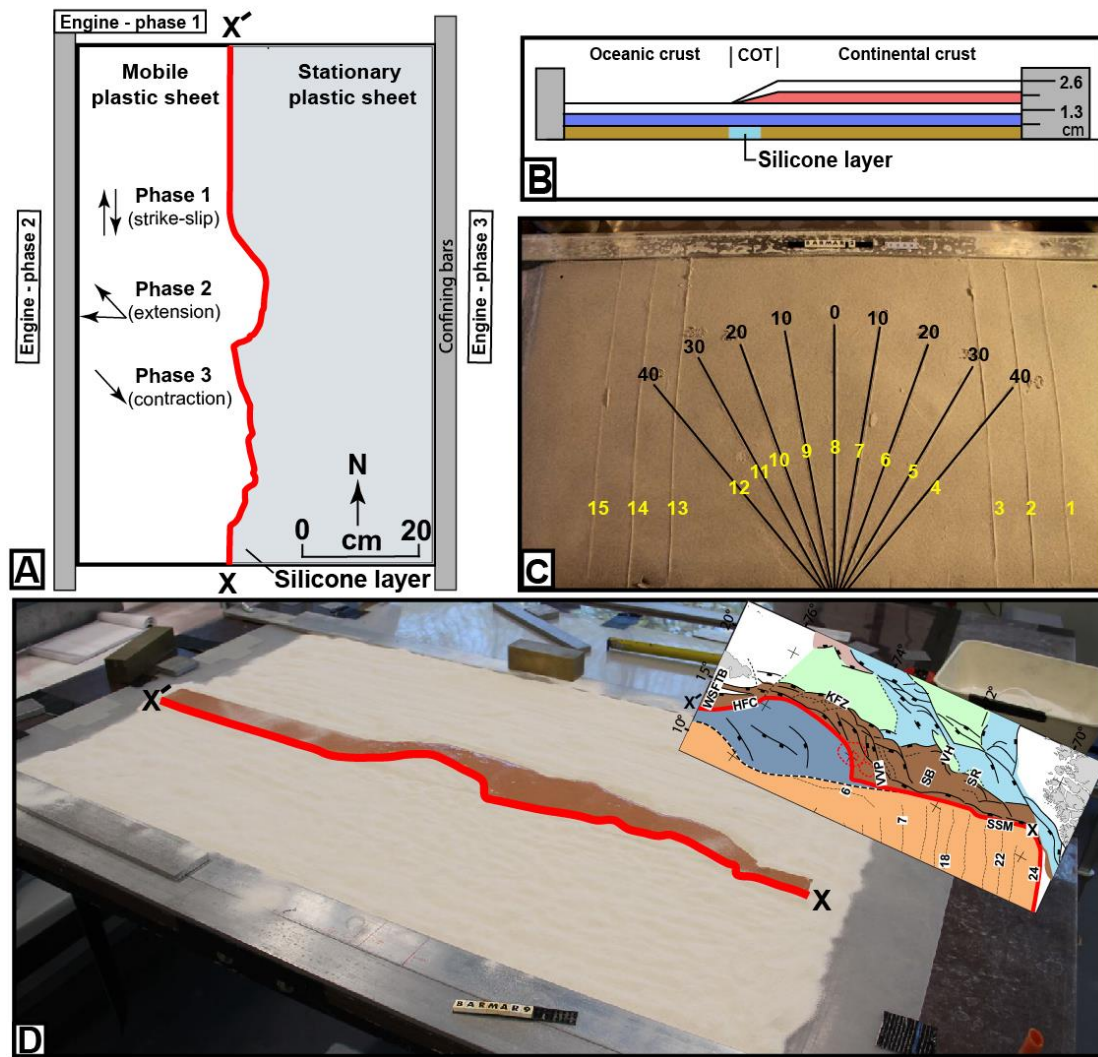
329 Several experimental studies have particularly focused on the geometry and  
330 development of pull-apart-basins in releasing bend settings (Mann et al., 1983;  
331 Faugère et al. 1983; Richard et al. 1995; Dooley & McClay 1997; Basile & Brun  
332 1999; Sims et al., 1999; Le Calvez & Vendeville, 2002; Mann, 2007; Mitra & Paul,  
333 2011). The pull-apart basin was described by Burchfiel & Stewart (1966) and  
334 Crowell (1974a,b) as formed at a releasing bend or at a releasing fault step-over  
335 along a strike-slip zone (Biddle & Christie-Blick 1985a,b). This basin type has also  
336 been termed “rhomb grabens” (Freund, 1971) and “strike-slip basins” (Mann et  
337 al., 1993) and is commonly considered to be synonymous with the extensional  
338 strike-slip duplex (Woodcock & Fischer, 1986; Dooley & Schreurs, 2012). In the  
339 descriptions of our experiments, we found it convenient to distinguish between  
340 extensional strike-slip duplexes in the context of Woodcock & Fischer (1986) and  
341 Twiss & Moores, 2007, p. 140-141;) and pull-apart basins (rhomb grabens:  
342 Crowell, 1974a,b; Aydin & Nur, 1993) since they reflect slightly different stages in  
343 the development in our experiments (see discussion).

344

## 345 **Experimental setup**

346

347 To study the kinematics of complex shear margins, a series of analogue  
348 experiments were performed at the tectonic modelling laboratory (TecLab) of  
349 Utrecht University, The Netherlands. All experiments were built on two  
350 overlapping 1 mm thick plastic sheets (each 100 cm long and 50 cm wide) that  
351 were placed on a flat, horizontal table surface. The boundary between the  
352 underlying movable and overlaying stationary plastic sheets had the shape of the  
353 mapped continent-ocean boundary (COB; **Figure 1B**). The moveable sheet was



354

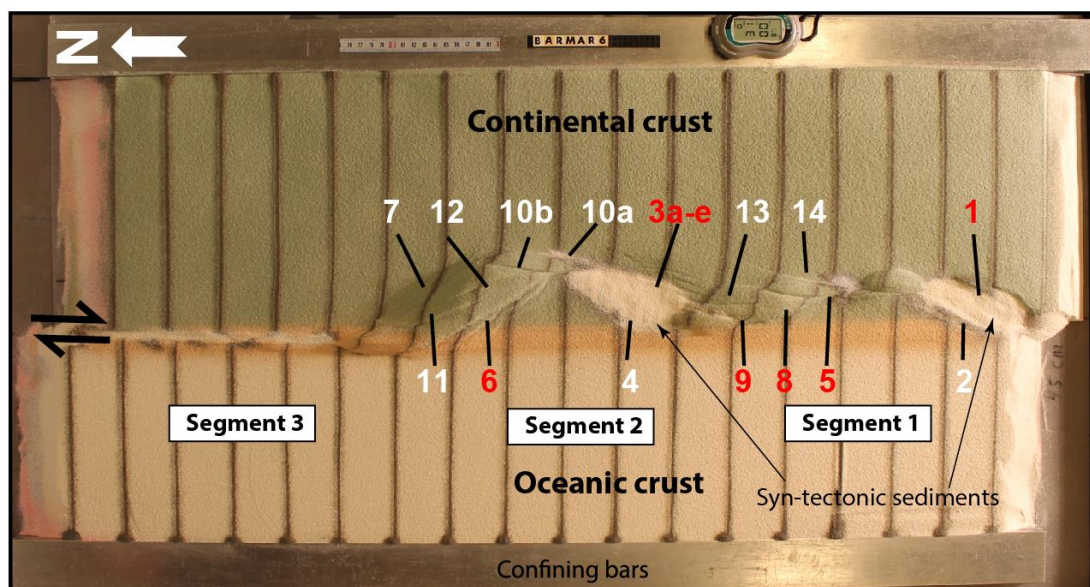
355 **Figure 3:** A) Schematic set-up of BarMar3-experiment as seen in map view. B) 356  
 357 Section through same experiment before deformation, indicating stratification  
 358 and thickness relations. C) Standard positions and orientation for sections cut in  
 359 all experiments in the BarMar-series. Yellow numbers are section numbers. Black  
 360 numbers indicate angle between the margins of the experiment (relative to N-S)  
 361 for each profile. D) Outline of silicone putty layer as applied in all experiments.  
 362 Inset shows original structural map of the Barents Margin used to define the width  
 363 of the thinned crust (same as Fig. 1B). Red line (X-X') indicates the western limit  
 364 of the thinned zone.

365 connected to an electronic engine, which pulled the sheet at constant velocity  
 366 during all three deformation stages. Displacement rates were therefore not scaled.  
 367 The modelling material was then placed on these sheets where the layers on the  
 368 stationary sheet represent the continental crust including the continent-ocean  
 369 transition (COT) whereas those on the mobile sheet represents the oceanic crust.  
 370 The model layers were confined by aluminum bars along the long sides and sand  
 371 along the short sides (**Figure 3A**). The continental crust tapers off towards the



372 oceanic crust with a relatively constant gradient. A sand-wedge with a constant  
373 dip angle determined by the difference in thickness between the intact and the  
374 stretched crust, and that covered the width of the silicon putty layer, was made to  
375 simulate the continent-ocean transition (**Figure 3B**). The taper angle was kept  
376 constant for all models.

377 The pre-cut shape of the plate boundary includes major releasing bends  
378 positioned so that they correspond to the geometry of the COB and the three main  
379 structural segments of the Barents Shear Margin as follows. *Segment 1* of the  
380 BarMar-experiments (**Figure 4**) contained several sub-segments with releasing  
381 and restraining bends as well as segments of “neutral” (Wilcox et al., 1973; Mann  
382 et al. 1983; Biddle & Christie-Blick, 1985b) or “pure” (Richard et al., 1991) strike-  
383 slip. *Segment 2* had a basic crescent shape, thereby defining a releasing bend at its  
384 southern margin in the position similar to that of the Vestbakken Volcanic  
385 Province that merged into a neutral shear-segment along the strike of, whereas a  
386 restraining bend occupied the northern margin of the segment. *Segment 3* was a  
387 straight basement segment, defining a zone of neutral shear and corresponds to  
388 the strike-slip segment west of Svalbard (**Figure 1**).



389  
390 **Figure 4:** Position of segments and major structural elements as referred to in the  
391 text and subsequent figures (see particularly **Figures 5 and 6**). This example is  
392 taken from the reference experiment BarMar6. All experiments BarMar6-9  
393 followed the same pattern, and the same nomenclature was used in the  
394 description of all experiments and provides the template for the definition of  
395 structural elements in Figure 7.  
396

397 The experiments included three stages of deformation with constant rates of  
398 movement of the mobile sheet at  $10 \text{ cmhr}^{-1}$  in all three stages. The relative angles  
399 of plate movements in the experiments were taken from post-late Paleocene  
400 opening directions in the northeast Atlantic (Gaina et al. 2009). Dextral shear was  
401 applied in the *first phase* in all experiments by pulling the lower plastic sheet by 5  
402 cm. In the *second phase* the left side of the experiment was extended by 3 cm  
403 orthogonally (BarMar6) or obliquely (325 degrees; BarMar 8 & 9) to the trend of  
404 the shear margin, whereas plate motion was reversed during the *third phase of*  
405 *deformation*, leading to inversion of earlier formed basins that had been  
406 developed in the strike-slip and extensional phases. Sedimentary basins that  
407 develop due to strike-slip (phase 1) or extension (phase 2) have been filled with  
408 layers of colored feldspar sand by sieving, so that a smooth surface was obtained.  
409 These layers are primarily important for discriminating among deformation  
410 phases and thus act as marker horizons. Phase 3 was initiated by inverting the  
411 orthogonal (BarMar6) or oblique (BarMar 8 & 9) extension of Phase 2 as a proxy  
412 for ridge-push that likely was initiated when the mid-oceanic ridge was  
413 established in Miocene time in the North Atlantic (Moser et al., 2002; Gaina et al.,  
414 2009). Contraction generated by ridge-push has been inferred from the mid-  
415 Norwegian continental shelf (Vågnes et al., 1998; Pascal & Gabrielsen, 2001;  
416 Faleide et al., 2008; Gac et al., 2016) and seems still to prevail in the northern areas  
417 of Scandinavia (Pascal et al., 2005), although far-field compression generated by  
418 other processes have been suggested (eg. Doré & Lundin, 1996).

419

420 Coloured layers of dry feldspar sand represent the brittle oceanic and continental  
421 crust. This material has proven suitable for simulating brittle deformation  
422 conditions (Willingshofer et al., 2005; Luth et al., 2010; Auzemery et al., 2021) and  
423 is characterized by a grain size of 100-200  $\mu\text{m}$ , a density of  $1300 \text{ kgm}^{-3}$ , a cohesion  
424 of  $\sim 16\text{-}45 \text{ Pa}$  and a peak friction coefficient of 0.67 (Willingshofer et al., 2018).  
425 Additionally, a 8 mm thick and of variable width corresponding to the COT (as  
426 mapped in reflection seismic data) of 'Rhodorsil Gomme GSIR' (Sokoutis, 1987)  
427 silicone putty mixed with fillers was used as a proxy for the thinned and weakened  
428 continental crust at the continent-ocean transition (**Figure 1B and 3A,B**). This



429 Newtonian material ( $n=1.09$ ) has a density of  $1330 \text{ kgm}^{-3}$  and a viscosity of  
430  $1.42 \times 10^4 \text{ Pa.s}$ .

431

432 The experiments have been scaled following standard scaling procedures as  
433 described by Hubbert (1937), Ramberg (1967) or Weijermars and Schmeling  
434 (1986), assuming that inertia forces are negligible when modelling tectonic  
435 processes on geologic timescales (see Ramberg (1981) and Del Ventisette et al.  
436 (2007) for a discussion on this topic). The models were scaled so that 10 mm in  
437 the model approximates c. 10 km in nature yielding a length scale ratio of  $1.00 \times 10^{-6}$ .  
438 As such, the model oceanic and continental crusts scale to 18 and 26 km in nature,  
439 respectively. A 26 km thick continental crust is a representative average for the  
440 crustal thickness east of the COT, ranging between 20 km in the SW Barents Sea  
441 and 30-32 km in the NW Barents Sea (Clark et al., 2012; Breivik et al. 2003). A  
442 thinning from 26 to 18 km across the COT is also realistic, however, the oceanic  
443 crust in the Norwegian-Greenland Sea is thinner than in the scaled model (Libak  
444 et al., 2012a,b).

445

446 The brittle crust, dry feldspar sand, deforms according to the Mohr-Coulomb  
447 fracture criterion (Horsfield, 1977; Mandl et al., 1977; McClay, 1990; Richard et  
448 al., 1991; Klinkmüller et al., 2016), whereas silicone putty promotes ductile  
449 deformation and folding. The geometry applied in the present experiments is  
450 accordingly well suited for the study of the COB/COT in the Barents Shear Margin  
451 (Breivik et al., 1998).

452

453 When complete, the experiments were covered with a thin layer of sand further to  
454 stabilize the surface topography before the models were saturated with water and  
455 cross-sections that were oriented transverse to the velocity discontinuity were cut  
456 in a fan-shaped pattern (**Figure 3C**). All experiments have been monitored with a  
457 digital camera providing top-view images at regular time intervals of one minute.

458

459 All experiments performed were oriented in a N-S-coordinate framework to  
460 facilitate comparison with the western Barents Sea area and had a three-stage  
461 deformation sequence (dextral shear – opening – closure). All descriptions and

462 figures relate to this orientation. It was noted that all experiments reproduced  
463 comparable basic geometries and structural types, demonstrating robustness  
464 against variations in contrasting strength of the “continent-ocean”-transition  
465 zone, which included a zone of silicone putty with variable width below an  
466 eastward thickening sand-wedge (**Figure 3B**) and changing displacement  
467 velocities.

468

## 469 **Modelling Results**

470

471 A series of nine experiments (BarMar1-9) with the set-up described above was  
472 performed. Experiments BarMar1-5 were used to calibrate and optimize  
473 geometrical outline, deformation rate, and angles of relative plate movements and  
474 are not shown here. The optimized geometries and experimental conditions  
475 utilized for experiments BarMar6-9, of which BarMar6 and 8 (and some examples  
476 from BarMar9) are illustrated here, yielded similar results in that all crucial  
477 structural elements (faults and folds) were reproduced in all experiments as  
478 described in the text and shown in **Figure 4**. It is emphasized that the extensional  
479 basins affiliated with the extension phase (phase 2) became wider in the  
480 orthogonal (BarMar6) as compared to oblique extension experiments (BarMar 8)  
481 (**Figures 5 and 6**). Furthermore, the fold systems generated in the experiments  
482 that utilized oblique contraction of  $325/145^{\circ}$  (BarMar8-9) produced more  
483 extensive systems of non-cylindrical folds with continuous, but more curved fold  
484 traces as compared to experiments with orthogonal extension/contraction  
485 (BarMar6). The fold axes generally rotated to become parallel to the (extensional)  
486 master faults delineating the pull-apart basins generated in deformation stage 1  
487 in experiments with an oblique opening/closing angle. Examples of the sequential  
488 development is displayed in **Figures 5 and 6**) and summarized in **Figure 7**.

489

490 Elongate positive structural elements with fold-like morphology as seen on the  
491 surface were detected during the various stages of the present experiments. The  
492 true nature of those were not easily determined until the experiments were  
493 terminated and transects could be examined. Such structures included buried  
494 push-ups (*sensu* Dooley & Schreurs, 2012), antiformal stacks, back-thrusts,

495 positive flower structures, fold trains, and simple anticlines. For convenience, we  
496 use the non-genetic term “positive structural elements” termed *PSE-m-n* for such  
497 structure types as seen in the experiments in the following description. In the  
498 following the deformation in each segment is characterized for the three  
499 deformation phases (**Table 1**).

500

### 501 **Deformation phase 1: Dextral shear stage**

502

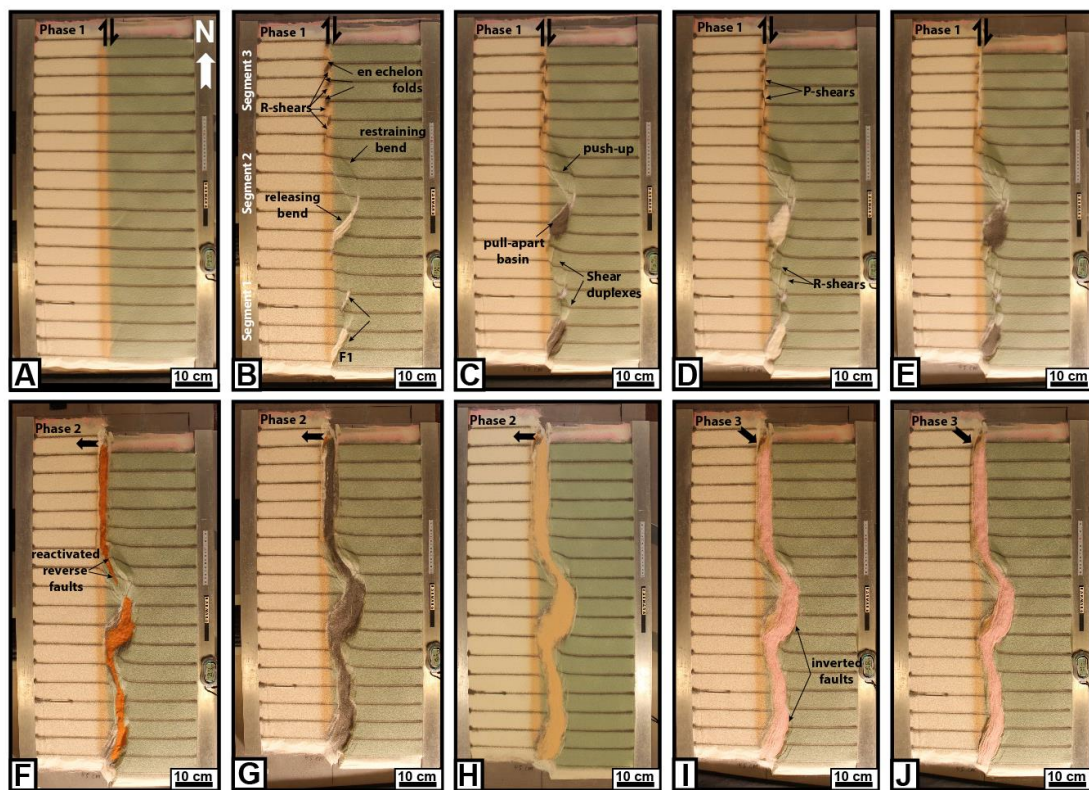
503 *Segment 1:* Differences in the geometry of the pre-cut fault trace between  
504 segments 1, 2 and 3 became evident after the very initial deformation stage.  
505 Particularly in segments 1 and 3 an array of oblique *en échelon* folds in between  
506 Riedel shear structures (*PSE-1-structures*) oriented c. 135° (NW-SE) to the  
507 regional VD rotating towards NNW-SSE by continued shear (**Figure 8**; see also  
508 Wilcox et al., 1973; Ordonne & Vialon, 1983; Richard et al., 1991; Dooley &  
509 Schreurs, 2012). These were simple, harmonic folds with upright axial planes and  
510 fold axial traces extending a few cm beyond the surface shear-zone described  
511 above. They had amplitudes on the scale of a few millimeters and wavelengths on  
512 scale of 5 cm. The *PSE-1-structures* interfered with or were dismembered by  
513 younger structures (Y-shears and *PSE-2-structures*; see below) causing northerly  
514 rotation of individual intra-fault zone lamellae (remnant *PSE-1-structures*; **Figure**  
515 **8**). Structures similar to *PSE-1-fold* arrays are known from almost all strike-slip  
516 experiments reported and described in the literature from the early works of (eg.  
517 Cloos, 1928; Riedel, 1929. See Dooley & Schreurs, 2012 for summary) and are  
518 therefore not given further attention here.

519

520 By 0.25 cm of horizontal displacement in segment 1, which included releasing and  
521 restraining bends separated by a central strand of neutral shear, a slightly  
522 curvilinear surface trace of a NE-SW-striking, top-NW normal faults in the  
523 southernmost part of segment 1 developed. This co-existed with the *PSE-1-*  
524 *structures* and was immediately paralleled by a normal fault with opposite throw  
525 (fault 2, **Figure 4**) so that the two faults constrained a crescent- or spindle-shaped  
526 incipient extensional shear duplex (**Figures 5B and 6B**; see also Mann et al., 1983;  
527 Christie-Blick & Biddle, 1985; Mann 2007; Dooley & Schreurs, 2012).

528

529 A system of *en échelon* faults separate N-S to NNE-SSE- striking normal and shear  
530 fault segments became visible in segment 1 after ca. 1 cm of shear (**Figure 5C,D**).  
531 These faults did not have the orientations as expected for R (Riedel) - and R' (anti-  
532 Riedel)- shears (that would be oriented with angles of approximately 15 and 75°  
533 from the master fault trace) but became progressively linked by along-strike  
534 growth and the development of new faults and fault segments. They thereby  
535 acquired the characteristics of Y-shears (oriented sub-parallel to the master fault  
536 trace), dissecting the PSE-1-structures. By 2.4 cm of shear, segment 1 had become  
537 one unified fault array (**Figures 5D and 6D**), delineating a system of incipient  
538 push-ups or positive flower structures (*PSE-2-structures*; **Figures 8 and Figure**  
539 **10, sections B1 and B3**, see also; Riedel, 1929; Wilcox et al., 1973; Odonne &  
540 Vialon, 1983; Dauteuil & Mart, 1995; Dooley & Schreurs, 2012).

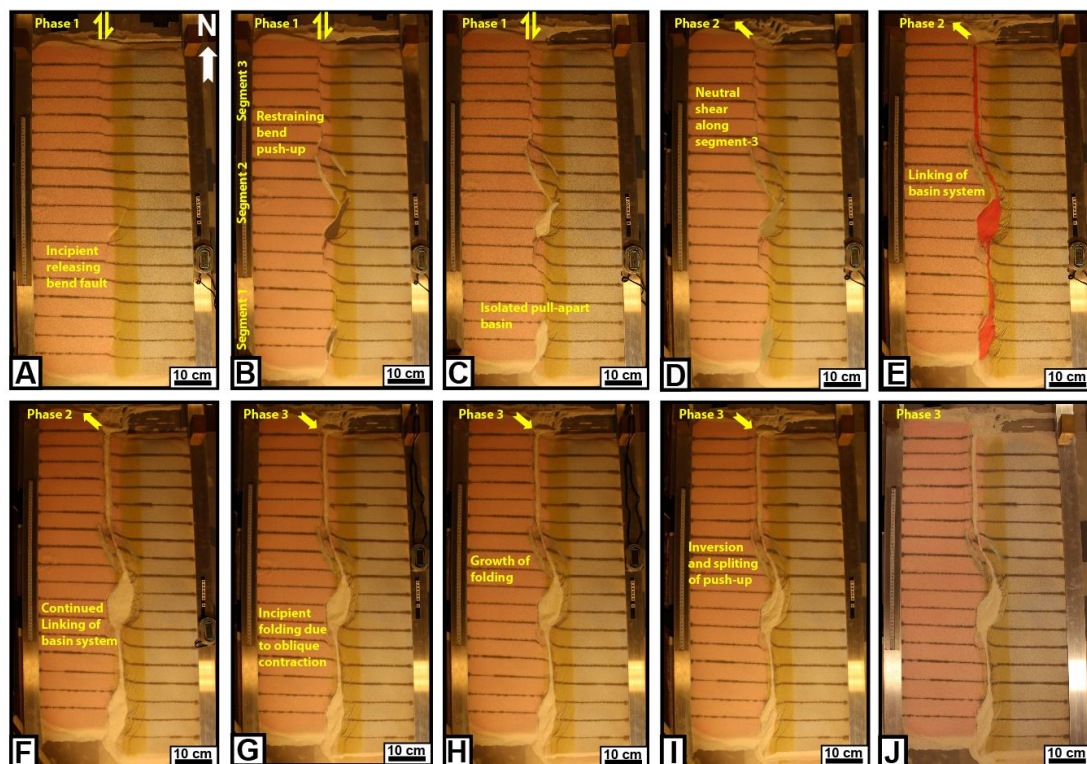


541

542

543 **Figure 5:** Sequential development of experiment BarMar6 by 0.5, 2.4, 3.5, 4.0 and  
544 5.0 cm of dextral shear (Steps A-E), orthogonal extension (steps F-H) and oblique  
545 contraction (steps I-J). The master fault strands are numbered in **Figure 4**, and  
546 the sequential development for each structural family is shown in **Figure 7**.  
547

548 The PSE-2-structures had amplitudes of 1 - 2 cm and wavelengths of 3 - 5 cm as  
 549 measured on the surface with fault surfaces that steepened down-section, the  
 550 deepest parts of the structures having cores of sand-layers deformed by open to  
 551 tight folds. The folds had upright or slightly inclined axial planes, dipping up to  
 552 55°, mainly to the east. The structures also affected the shallowest layers down to  
 553 1-2 cm in the sequence, but the shallowest sequences were developed at a later  
 554 stage of deformation and were characterized by simple gentle to open anticlines.  
 555 These structures were constrained to a zone of deformation directly above the  
 556 trace of the basement fault, similar to that commonly seen along shear zones (e.g.  
 557 Tchalenko, 1971; Crowell, 1974 a,b; Dooley & Schreurs, 2012). This zone was 3-4  
 558 cm wide and remained stable throughout deformation stage 1 and was restricted  
 559



560

561 **Figure 6:** Sequential development of experiment BarMar8 by 1.0, 3.5 and 5.0 cm  
 562 of dextral shear (Steps A-C), oblique extension (steps D-F) and oblique contraction  
 563 (steps G-I). Step J represents the final model after end of contraction. The master  
 564 fault strands are numbered in **Figure 3**, and the sequential development for each  
 565 structural family is shown in **Figure 7**. Phases 2 and 3 involved oblique ( $325^{\circ}$ )  
 566 extension and contraction in this experiment.  
 567

568 to the close vicinity of the basement shear fault itself as also described from one-  
 569 stage shear faults in Riedel box-type experiments (e.g. Tchalenko, 1970; Naylor et

570 al., 1986; Richard et al., 1991; Casas et al., 2001; Dauteuil & Mart, 1998; Dooley &  
571 Schreurs, 2012) and from nature as well (e.g. Wilcox et al., 1973; Harding, 1974;  
572 Harding & Lowell, 1979; Sylvester, 1988; Woodcock & Schubert, 1994; Mann,  
573 2007).

574

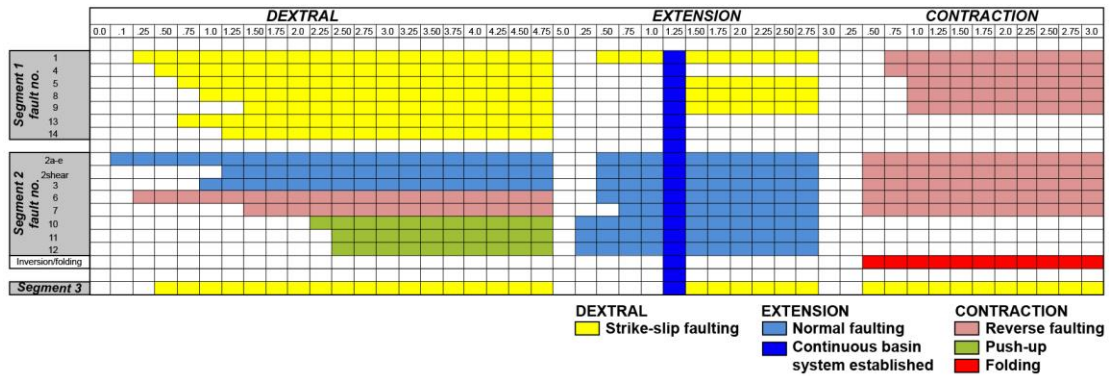
575 A horse-tail-like fault array developed by ca. 3 cm of shear at the transitions  
576 between segments 1 and 2 (see also Cunningham & Mann, 2007; Dooley &  
577 Schreurs, 2012, their Figure 44) (**Figures 5B-D and 6B-D**).

578 The structuring in *Segment 2*; was ruled by the crescent-shaped basement fault  
579 (VD) that generated a releasing bend along its southern and a restraining bend  
580 along its northern border (**Figure 11**). The first fault of fault array 3a-e in the  
581 southern part of Segment 2 was activated after c. 0.15 cm of bulk horizontal  
582 displacement (**Figure 7**). It was situated directly above the southernmost pre-cut  
583 releasing bend, defining the margin of crescent-shaped incipient extensional  
584 strike-slip duplexes (in the context of Woodcock & Fischer, 1986, Woodcock &  
585 Schubert, 1994 and Twiss & Moores, 2007, p. 140-141). The developing basin got  
586 a spindle-shaped structure and developed into a basin with a lazy-S-shape  
587 (Cunningham & Mann, 2007; Mann, 2007). The basin widened towards the east by  
588 stepwise footwall collapse, generating sequentially rotating crescent-shaped  
589 extensional fault blocks that became trapped as extensional horses in the footwall  
590 of the releasing bend (**Figure 11**). In the areas of the most pronounced extension,  
591 the crestal part of the rotational fault blocks became elevated above the basin  
592 floor, generating ridges that influenced the basin floor topography and hence, the  
593 sedimentation. By continued rotation of the fault blocks and simultaneous sieving  
594 of sand the crests of the blocks became sequentially uplifted, generating forced  
595 folds (Hamblin, 1965; Stearns, 1978; Groshong, 1989; Khalil & McClay, 2016)  
596 (**Figure 10A**). In the analysis we used the term *PSE-3-structures* for these  
597 features. Simultaneously, an expanding sand-sequence became trapped in the  
598 footwalls of the master faults, defining typical growth-fault geometries.

599

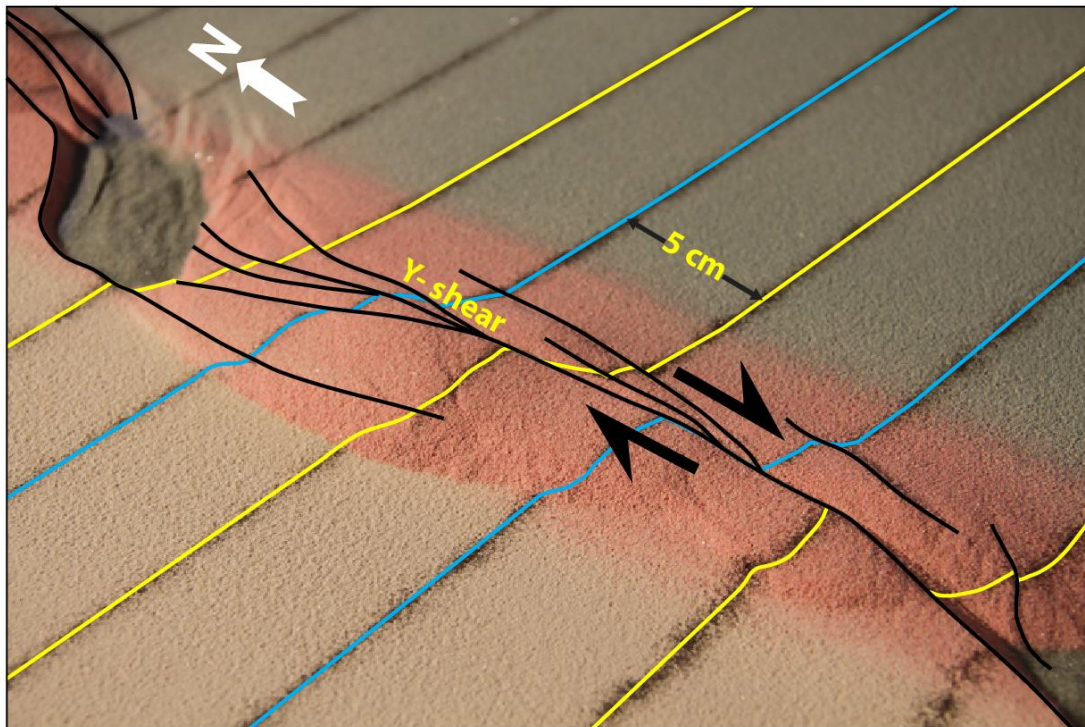
600 By a shear displacement of 0.55 cm additional curved splay faults were initiated  
601 from the northern tip of the master fault of fault 3f; **Figure 7**), delineating the  
602 northern margin of a rhombohedral pull-apart-basin (Mann et al., 1983; Mann,





603

604 **Figure 7:** Summary of sequential activity in each master structural element  
 605 **(Figure 4)** in Experiment BarMar6 **(Figure 5)**. Type and amount of displacement  
 606 is shown in two upper horizontal rows. The vertical blue bar indicates the stage at  
 607 which full along-strike communication became established between marginal  
 608 basins. Color code (see in-set) indicates type of displacement at any stage.  
 609



610

611 **Figure 8:** PSE-1 anticline-syncline pairs in segment 1 experiment BarMar6 in an  
 612 oblique view. PSE-1 folds were constrained to the very fault zone and the fold axes  
 613 (blue lines) and extended only 3-4 cm beyond the fault zone. PSE-2 structures  
 614 (incipient shear-duplex and positive flower structures; yellow lines) were  
 615 delineated by shear faults and completely cannibalized PSE-1 structures by  
 616 continued shear. Yellow and blue lines show the rotation of the fold axial trace  
 617 caused by dextral shearing of c. 1,5 cm. 25mm of dextral shear. By a displacement  
 618 of 35mm the remains of the PSE-1 structure was completely obliterated. The  
 619 distance between the markers (dark lines) is 5cm. Yellow arrow marks north-  
 620 direction. White arrows indicate shear direction.  
 621

622 2007; Christie-Blick & Biddle, 1985) and with a geometry that was  
623 indistinguishable from pull-apart basins or rhomb grabens affiliated with  
624 unbridged *en échelon* fault arrays (Crowell, 1974 a,b; Aydin & Nur, 1993).  
625 Although sand was filled into the subsiding basins to minimize the graben relief  
626 and to prevent gravitational collapse, the sub-basins that were initiated in the  
627 shear-stage were affected by internal cross-faults, and the initial basin units  
628 remained the deepest so that the buried internal basin topography maintained a  
629 high relief with several apparent depocenters separated by intra-basinal  
630 platforms.

631

632 Systems of linked shear faults and PSE-structures became established in the  
633 central part with neutral shear that separate the releasing and restraining bends  
634 and development similarly to that seen for segment 3 (see below). However, these  
635 structures were soon destroyed by the combined development of the northern  
636 and southern tips of the extensional and contractional shear duplexes (**Figure**  
637 **10**).

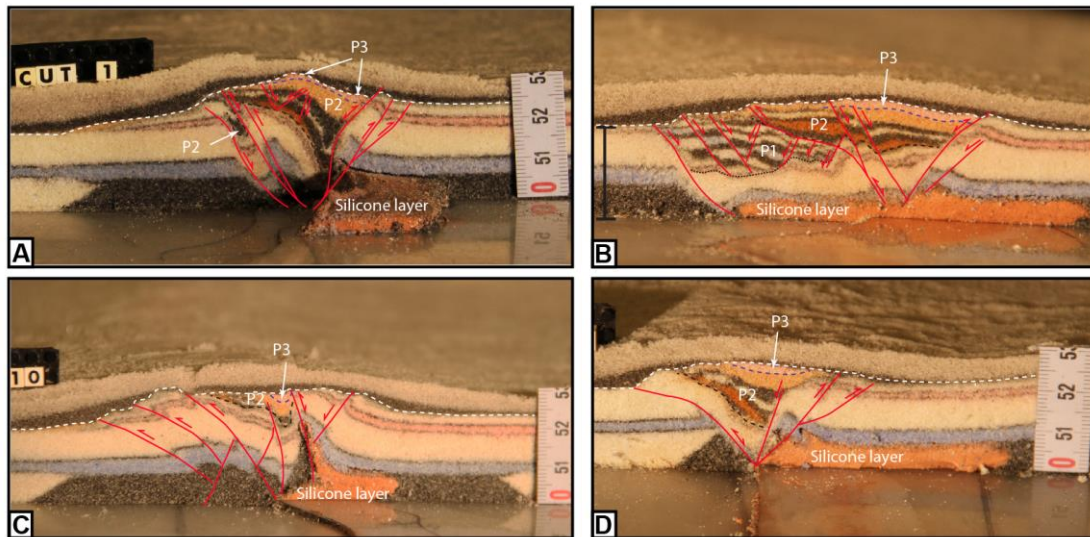
638

639 The first structure to develop in the regime of the restraining bend (segment 2;  
640 was a top-to-the-southwest (antithetic) thrust fault at an angle of  $145^{\circ}$  with the  
641 regional trend of the basement border as defined by segments 1 and 3 (Fault 6). It  
642 became visible by 0.5 cm of displacement. The northern part of segment 2 became,  
643 however, dominated by a synthetic contractional top-to-the-northeast fault that  
644 was initiated by 0.85 cm of shear (Fault 7; **Figures 5 and 6**). Thus, faults 6 and 7  
645 delineated a growing half-crescent-shaped 5-7-cm wide push-up structure (Aydin  
646 & Nur, 1982; Mann et al., 1983) south of the restraining bend (**Figure 9**; *PSE-4-*  
647 *structures*). By continued shear these structures got the character of an antiformal  
648 stack.

649

650 *Segment 3* defined a straight strand of neutral shear. Its development in the  
651 BarMar-experiments followed strictly that known from numerous published  
652 experiments (e.g., Tchalenko, 1970; Wilcox et al., 1973; Harding, 1974; Harding &  
653 Lowell, 1979; Naylor et al., 1986; Sylvester, 1988; Richard et al., 1991; Woodcock  
654 & Schubert, 1994; Dauteuil & Mart, 1998; Mann, 2007; Casas et al., 2001; Dooley

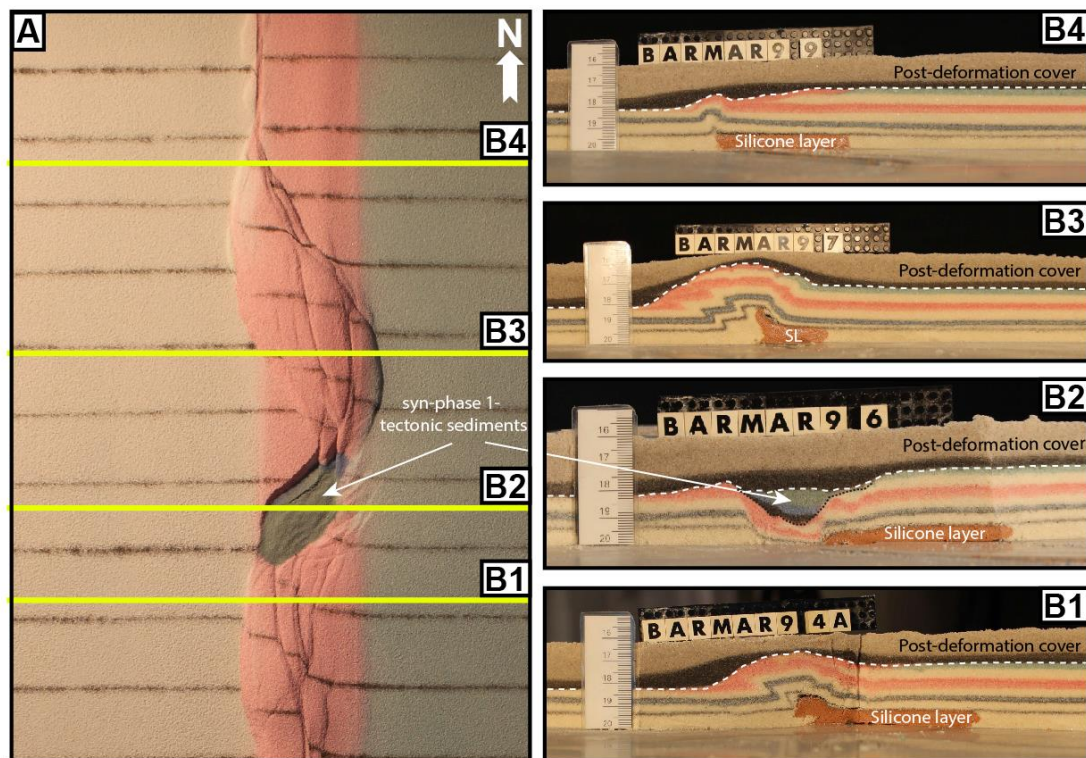




655

656 **Figure 9:** Cross-sections through PSE-2-related structures. **A)** Folded core of  
 657 incipient push-up/positive flower structure in segment 1, experiment BarMar6.  
 658 The fold structure is completely enveloped of shear faults that have a twisted  
 659 along-strike geometry. Note that the eastern margin of the structure developed  
 660 into a negative structure at a late stage in the development (filled by black-pink  
 661 sand sequence) and that the silicone putty sequence (basal pink sequence) was  
 662 entirely isolated in the footwall. **B)** Similar structure in experiment BarMar8. The  
 663 weak silicone putty layer here bridged the high-strain zone and focused folding  
 664 that propagated into the sand layers (blue). The folds in upper (pink layers) were  
 665 associated with the contraction stage, because they contributed to a surface relief  
 666 filled in by red-black-sand sequence that was sieved into the margin during the  
 667 contraction stage. **C)** Contraction associated with “crocodile structure” in the  
 668 footwall of the main fault in segment 1, experiment BarMar8. Note disharmonic  
 669 folding with contrasting fold geometries in hanging wall and footwall and at  
 670 different stratigraphic levels in the footwall, indicating shifting stress situation in  
 671 time and space in the experiment. **D)** Transitional fault strand between to more  
 672 strongly sheared fault segments (experiment BarMar9).  
 673

674 & Schreurs, 2012). A train of Riedel-shears, occupying the full length of the  
 675 segment, appeared simultaneously on the surface after a shear displacement of  
 676 0.5 cm, occupying a restricted zone with a width of 2-3 cm. The Riedel-shears  
 677 dominated the continued structural development of Segment 3. Riedel'-shears  
 678 were absent throughout the experiments, as should be expected for a sand-  
 679 dominated sequence (Dooley & Schreurs, 2012). P-shears developed by continued  
 680 shear, creating linked rhombic structures delineated by the Riedel- and P-shears  
 681 generating positive structural elements with NW-SE- and NNE-SSE-striking axes  
 682 (see also Morgenstern & Tchalenko, 1967), soon coalescing to form Y-shears.  
 683 Transverse sections document that these structures were cored by push-up



684

685 **Figure 10: A)** contrasting structural styles along the master fault system in  
 686 segment 2 in map view and **(B)** cross sections of experiment BarMar9. SL denotes  
 687 silicone layer, the stippled line the boundary between pre- and syn-deformation  
 688 layers and the white dashed line the boundary with the post-deformation layers.  
 689

690 anticlines, positive half-flower structures and full-fledged positive flower  
 691 structures in the advanced stages of shear (*PSE-4-structures*) (**Figures 5 and 6.**  
 692 **See also Figure 10**). These were accompanied by the development of *en échelon*  
 693 folds and flower structures as commonly reported from strike-slip faults in nature  
 694 and in experiments. The width of the zone above the basal fault remained almost  
 695 constant throughout the experiments, but was somewhat wider in experiments  
 696 with thicker basal silicone polymer layers, similar to that commonly described  
 697 from comparable experiments (eg., Richard et al., 1991).

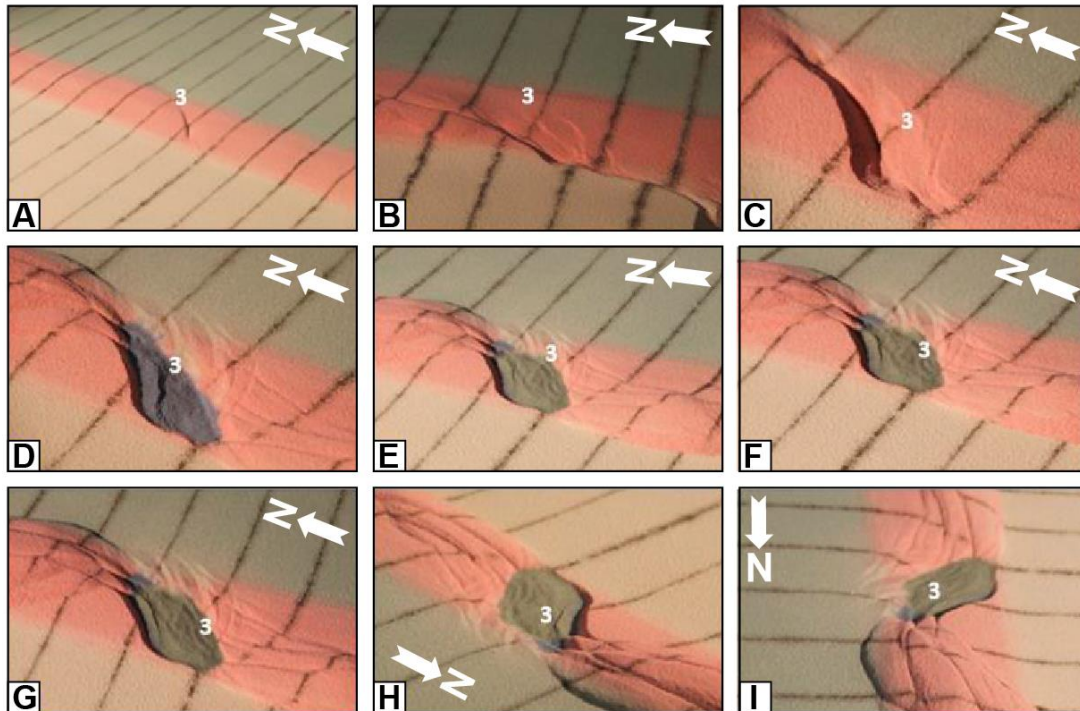
698

### 699 **Deformation Phase 2: Extension**

700

701 The Palaeogene dextral shear was followed by pure extension accompanying the  
 702 opening along the Barents Shear Margin in the Oligocene. Our experiments  
 703 focused on the effects of oblique extension, acknowledging that plate tectonic

704



705

706 **Figure 11:** Nine stages in the development of the extensional shear duplex system  
 707 above the releasing bend in experiment BarMar9. The master faults that  
 708 developed at an incipient stage (e.g., Fault 3 that constrained the eastern margin  
 709 of the extensional shear duplex) remained stable and continued to be active  
 710 throughout the experiment (Figure 7), but became overstepped by faults in its  
 711 footwall that became the basin contraction faults at the later stages H and I. Note  
 712 that the developing basement was stabilized by infilling of gray sand during this  
 713 part of the experiment. Note that Fault 3 remained active and broke through the  
 714 basin infill also after the basin infill overstepped the original basin margin. The  
 715 distance between the markers (dark lines) is 5cm. Yellow arrow marks north-  
 716 direction. Note that figure I has a different orientation.

717

718 reconstructions of the North Atlantic suggest an extension angle of  $325^\circ$  as the  
 719 most likely (Gaina et al., 2009).

720

721 All strike-slip basins widened in the extensional stage, and most extensively so for  
 722 the experiments with orthogonal extension. The widening of the basin enhanced  
 723 the topography already generated in the shear-stage in the extensional strike-slip  
 724 duplex in segment 2 (PSE-3-structures). In the earliest extensional stage the  
 725 strike-slip basin in segment 2 dominated the basin configuration, but by continued  
 726 extension the linear segments and the minor pull-apart basins in segments 1 and  
 727 2 started to open and became interlinked, subsequently generating a linked basin  
 728 system that paralleled the entire shear margin (**Figures 5F-G, 6F-G**).



729

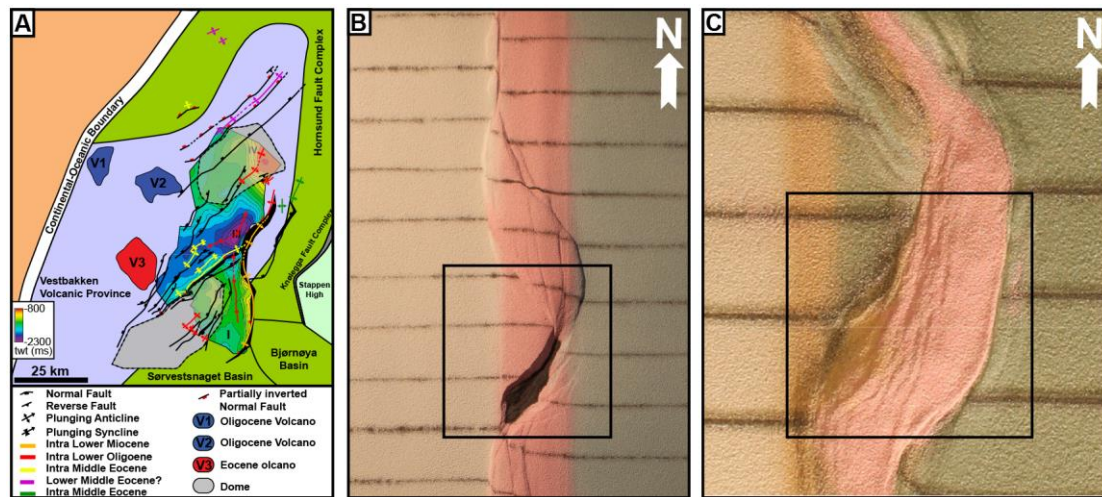
730 The extension-phase following dextral strike-slip reactivated and very quickly  
731 linked several of the master faults that were established in deformation phase 1  
732 (**Figures 5A and 6A**) already by an extension of 0,25 – 0,50 cm. This included the  
733 southern fault margin, the push-up and the splay faults defining a crestral collapse  
734 graben of the push-up (Faults 6, 11 and 12; **Figure 4**). All three segments were  
735 reactivated in extension by c. 1.25 cm of orthogonal stretching (**Figure 7**). During  
736 the first cm of extension each basin remained an isolated unit, but after 1 cm of  
737 extension all basins became linked, thus forming one unified elongate extensional  
738 basin (marked by the vertical dark blue line in **Figure 7**) and mainly following the  
739 PDZ as it was cut in the basal templates. Among the faults that were inactive and  
740 remained so throughout the extension phase were the antithetic contractional  
741 fault delineating the push-ups in segment 2 towards the south (Fault 6; **Figure 4**).  
742 The Y-shear in Segment 3 was reactivated as a straight, continuous extensional  
743 fault in Stage 2. Total extension in Phase 3 was 5 cm.

744

### 745 **Deformation Phase 3: Contraction**

746

747 In our experiments the extension stage was followed by orthogonal or oblique  
748 contraction (parallel to the direction of extension as applied for each experiment).  
749 The experiments were terminated before the full closure of the basin system, in  
750 accordance with the extension vector > contraction vector as in the North Atlantic  
751 (see Vågnes et al., 1998; Pascal & Gabrielsen 2001; Gaina et al. 2009). A part of the  
752 early-stage contraction was accommodated along new faults. It was more  
753 common, however, that faults that had been generated in the strike-slip and  
754 extensional stages became reactivated and rotated, and the development of  
755 isolated folds, which were commonly associated with inverted fault traces,  
756 generating snakehead- or harpoon-type structures (Cooper et al., 1989; Coward,  
757 1994; Allmendinger, 1998; Yameda & McClay, 2004; Pace & Calamitra, 2014); *PSE-*  
758 *5-structures*). This was particularly the case for the master faults. The dominant  
759 structures affiliated with the contractional stage was still new folds with traces  
760 oriented orthogonal to the shortening direction and sub-parallel to the preexisting  
761 master fault systems that defined the margin and basin margins (**Figure 12**). Also,



762  
763  
764  
765  
766  
767  
768

**Figure 12:** PSE-5 and PSE-6 folds generated during phase 3-inversion, experiment BarMar8. Note that fold axes mainly parallel the basin rims, but that they deviate from that in the central parts of the basins in some cases. Note that the folds are best developed in segment 2, which accumulated extension in the combined shear and extension stages.

769  
770  
771  
772  
773  
774  
775  
776  
777  
778

some deep fold sets that had been generated during the strike-slip phase and seen as domal surface features became reactivated, causing renewed growth of surface structures (see **Figure 10** and explanation in figure caption). These folds were generally up-right cylindrical buckle folds in the initial contractional stage and with very large trace length: amplitude-ratio (*SPE-6-structures*). Some intra-basin folds, however, defined fold arrays that diagonally crossed the basins. Particularly the folds situated along the basin margins developed into fault propagation-folds above low-angle thrust planes. Such faults aligning the western basin margins could have an antithetic attitude relative to the direction of contraction.

779  
780  
781  
782  
783  
784  
785  
786  
787

During the contractional phase the margin-parallel, linked basin system started immediately to narrow and several fault strands became inverted. The basin-closure was a continuous process until the end of the experiment by 3 cm of contraction. The contraction was initiated as a proxy for an ESE-directed ridge-push stage. The first effect of this deformation stage was heralded by uplift of the margin of the established shear zone that had developed into a rift during deformation stage 2. This was followed by the reactivation and inversion of some master faults (e.g., fault a2; **Figure 4**) and thereafter by the development of a new set of low-angle top-to-the-ESE contractional faults. These faults displayed a

788 sequential development (**Figure 4**) and were associated with folding of the strata  
789 in the rift structure, probably reflecting foreland-directed in-sequence thrusting  
790 (PSE-5 and PSE-6 fold populations).

791

## 792 **Discussion**

793

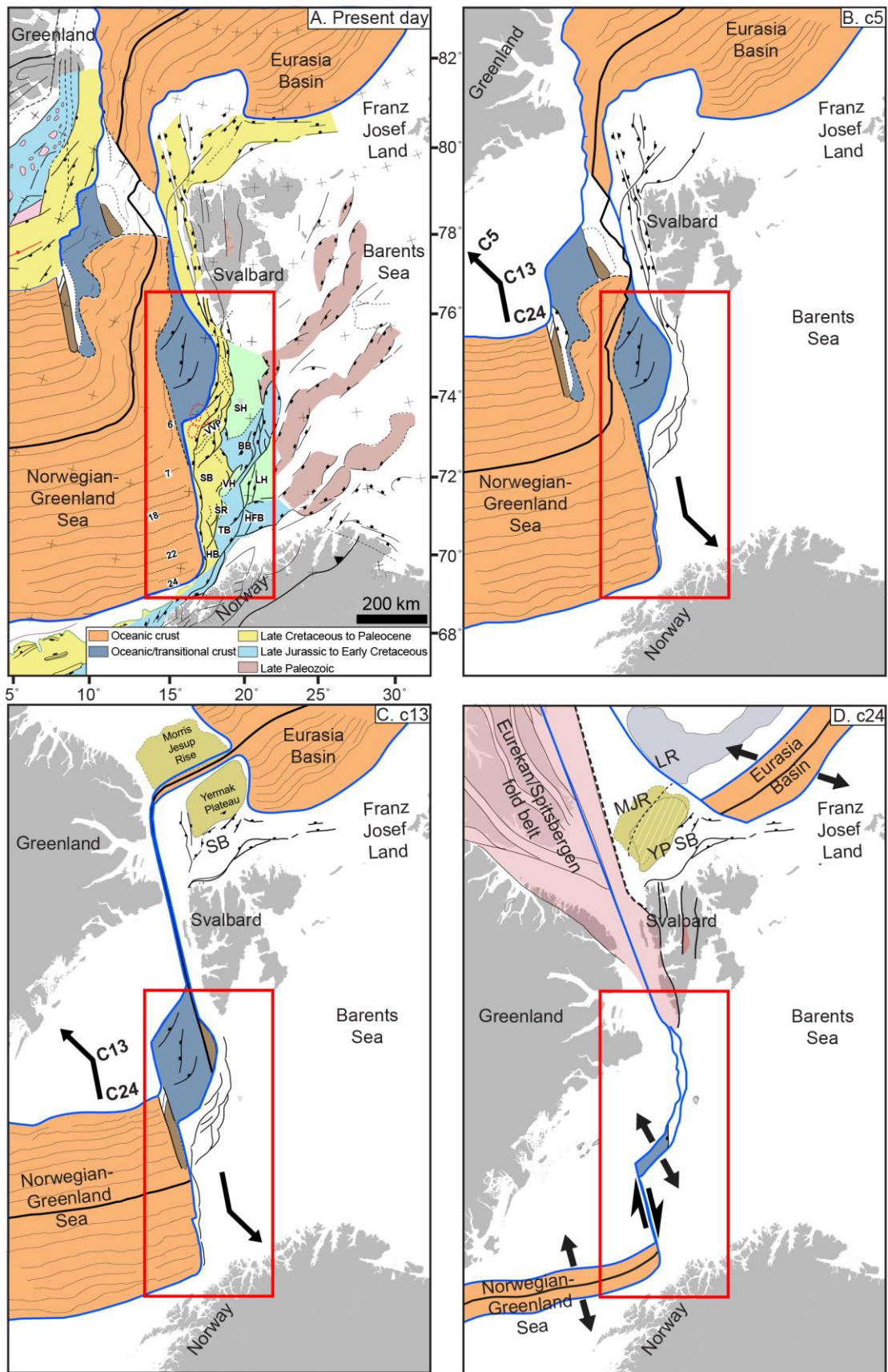
794 The break-up and subsequent opening of the Norwegian-Greenland Sea was a  
795 multi-stage event (**Figure 13**) that imposed shifting stress configurations  
796 overprinting the already geometrically complex Barents Shear Margin. Therefore,  
797 scaled experiments were designed to illuminate the structural development of the  
798 Barents Shear Margin. The experiments utilized three main segments that  
799 correspond to the Senja Fracture Zone (segment 1), the Vestbakken Volcanic  
800 Province (segment 2) and the Hornsund Fault Zone (segment 3). A series of  
801 structural families developed during the experiments, most of which correspond  
802 to structural elements found along the Barents Shear Margin.

803

804 Segment 1 in the experiments (which corresponds to the Senja Shear Margin) was  
805 dominated by neutral dextral shear, although subordinate jogs in the (pre-cut)  
806 fault provided minor sub-segments with mainly releasing and subordinate  
807 restraining bends. PSE-1-folds that developed at an incipient stage were  
808 immediately paralleled by two sets of normal faults with opposite throw in the  
809 releasing bend areas (e.g., fault 2; **Figure 4**). The two faults defined a crescent- or  
810 spindle-shaped incipient extensional shear duplex (**Figures 5B and 6B**; see also  
811 Mann et al., 1983; Christie-Blick & Biddle, 1985; Mann, 2007; Dooley & Schreurs,  
812 2012). The most prominent of these structures corresponds to the position of the  
813 Sørvestsnaget Basin (**Figure 1B**).

814

815 Counterparts to PSE-1 and PSE-2 structural populations observed in the  
816 experiments were not identified with certainty in the seismic data along the  
817 Barents Shear Margin, although some isolated, local anticlinal features could be  
818 dismembered remnants of such. The PSE-1 and PSE-2 structures generally belong  
819 to the structural populations that were developed at the earliest stages of the  
820 experiments. Furthermore, these structure types were confined to the area just



821

822 **Figure 13;** Main stages in opening of the North Atlantic. A) Present day, B) chron  
 823 5 (10 Ma in the late Miocene), C) chron 13 (33 Ma in the earliest Oligocene), D)  
 824 chron 24 (53 Ma in the early Eocene).

825 above the basal master fault (VD) and its immediate vicinity (see also experiments  
826 in series “e” and “f” of Mitra & Paul, 2011). Because of their constriction to the near  
827 vicinity of the master fault, we speculate that structures generated at an early  
828 stage of shear, are vulnerable to cannibalisation by younger structures with axes  
829 striking parallel to the main shear fault (Y-shears; SPE-2-structures). We therefore  
830 conclude that the majority of these structure populations were destroyed during  
831 the later stages of shear and during the subsequent stages of extension and  
832 contraction.

833

834 During the oblique extension stage segment 1 of experiments BarMar7-9 the basin  
835 subsidence was focused in the minor pull-apart basins, which soon became linked  
836 along the regional N-S-striking basin axis. Remains of several such basin centers,  
837 of which the Sørvestsnaget Basin (Knutsen & Larsen, 1997; Kristensen et al., 2017)  
838 is the largest, are preserved and found in seismic data (**Figure 1b**). During the  
839 experiments a continuous basin system was developed in the hangingwall side of  
840 the master fault, but it is not likely that opening occurred prior to the extension of  
841 the margin underlain by continental crust reached a stage where the separate  
842 basin units paralleling the Barents Shear Margin became linked.

843

844 In the subsequent inversion stage, fold trains with axial traces parallel (PSE-5-  
845 folds) to the basin axis and the master faults characterized segment 1. Remnants  
846 of such folds are locally preserved in the thickest sedimentary sequences affiliated  
847 with the Senja Shear Margin.

848

849 Segment 2, which was underlain by a crescent-shaped discontinuity corresponds  
850 to the Vestbakken Volcanic Province and the southern extension of the Knølegga  
851 Fault Complex that is a branch of the southern part of the Hornsund Fault Zone  
852 (**Figures 1b and 4**). The part of the Vestbakken Volcanic Province that was the  
853 subject of structural analysis by Giennenas (2018) corresponds to the southern  
854 part of segment 2 in the present experiments. It is dominated by interfering NNW-  
855 SSE- and NE-SW striking fold- and fault systems in the central part of the basins,  
856 whereas N-S-structures are more common along its eastern margin (**Figure 12A**)  
857 (Jebsen & Faleide, 1998; Giennenas, 2018).



858

859 Intra-basinal platforms and complex internal configurations seen in the BarMar-  
860 experiments are common in strike-slip basins (eg. Dooley & McClay, 1997; Dooley  
861 & Schreurs, 2012) and are consistent with the structural configuration with intra-  
862 basin depo-centers within the Vestbakken Volcanic Province and also in the  
863 Sørvestsnaget Basin (Knutsen & Larsen, 1997; Jebsen & Faleide, 1998; **Figure 13**).  
864 The positive structural elements that prevail in *segment 3* belong to the PSE-2-  
865 structure population. The structures affiliated with segment 3 in the BarMar-  
866 experiments are similar to those seen in the reflection seismic sections along parts  
867 of the Spitsbergen and the Senja shear margins (Myhre et al., 1982; Faleide et al.,  
868 1993). Thus, the structuring in the segment 3 in the BarMar-experiments display  
869 a configuration typical for neutral shear (Cloos, 1928; Riedel, 1929; Tchalenko,  
870 1970; Wilcox et al., 1973). *Én echelon* folds (corresponding to PSE-1-structures)  
871 first became visible, to be succeeded by the development of Riedel- and P-shears  
872 (R'-shears were subdued as expected for sand-dominated sequences (Dooley &  
873 Schreurs, 2012). Continued shear followed by collapse and interaction between  
874 Riedel and P-shears and the subsequent development of Y-shears initiated push-  
875 up- and flower-structures with N-S-axes (PSE-2), structures that were expressed  
876 as non-cylindrical (double-plunging) anticlines on the surface (e.g., Tchalenko,  
877 1970; Naylor et al., 1986). Structures similar to the PSE-2-structures that were  
878 initiated in the present experiments have previously been reported from similar  
879 experiments with viscous basal layers covered by sand (e.g. Richard et al., 1991;  
880 Dauteuil & Mart, 1998), illustrating the influence of a mechanical stratified  
881 sequence on fold configurations.

882

883 The Knølegga Fault Zone occupies a km-wide zone. The master fault strand is  
884 paralleled by faults with significant normal throws on its hanging wall side and  
885 this is considered to be strands belonging to the larger Knølegga Fault Complex  
886 (EBF; Eastern Boundary Fault; Giannenas, 2018; **Figure 12A**). The EBF zone is a  
887 top-west normal fault with maximum throw of nearly 2000 ms (3000 meters). It  
888 can be followed along its strike for more than 60 km and seems to die out by horse-  
889 tailing at its tip-points. The vicinity of the master faults of the Knølegga Fault  
890 Complex locally display isolated elongate positive structures constrained by

891 steeply dipping faults. These structures sometimes display internal reflection  
892 patterns that seem exotic or suspect in comparison to the surrounding sequences.  
893 Some of these structures resemble positive flower structures or push-ups or  
894 define narrow anticlines. They are found in both the footwall and hanging wall of  
895 the border faults and strike parallel to those and the axes of these structures  
896 parallel the master faults. The traces of such structures can be followed over  
897 shorter distances than the master faults, and do not occur in the central parts of  
898 the Vestbakken Volcanic Province. We speculate that these are rare fragments of  
899 dismembered PSE-1-type structures.

900

901 Due to the right-stepping geometry during dextral shear in segment 2, the  
902 southern and northern parts were in the releasing and restraining bend positions,  
903 respectively (e.g., Christie-Blick & Biddle, 1985). Hence, the southern part of  
904 segment 2 was subject to oblique extension, subsidence and basin formation when  
905 the northern part was subject to oblique contraction, shortening and uplift. The  
906 southern segment expanded to the east and northeast by footwall collapse and  
907 activation of rotating fault blocks that contributed to a basin floor topography that  
908 affected the pattern of sediment accumulation (**Figure 9A, B**). The crests of the  
909 rotating fault blocks are termed PSE-3-structures above, and such eroded fault  
910 block crests are defining the footwalls of major faults in the Vestbakken Volcanic  
911 Province, providing space for sediment accumulation in the footwalls. The area  
912 that was affected by the basin formation in the extensional shear duplex stage  
913 seems to have remained the deepest part of the Vestbakken Volcanic Province,  
914 whereas the part formed in basin widening by sequential footwall collapse created  
915 a shallower sub-platform (*sensu* Gabrielsen, 1986) (**Figure 11**). It is expected that  
916 (regional) basin and (local) fault block subsidence became accelerated during  
917 phase 2 (extension), and more so in the orthogonal extension experiments  
918 (BarMar 6) than in the experiments with oblique extension (BarMar 8), but due to  
919 stabilization of basins by infilling of sand, this was not documented. The widening  
920 occurred mainly by fault-controlled collapse of the footwalls, and dominantly  
921 along the master faults that correspond to the Knølegga Fault Zone, but also new  
922 intra-basin cross-faults that were initiated in the shear stage (see above) became  
923 reactivated, contributing to the complexity of the basin topography. It is not likely

924 that a stage was reached where all (pull-apart) basin units along the margin  
925 became fully linked, although sedimentary communication along the margin may  
926 have become established.

927

928 The contraction (phase 3) clearly reactivated normal faults, probably causing  
929 focusing of hanging wall strain and folding, rotation of fault blocks and steepening  
930 of faults. This means that both intra-basinal and marginal faults in the Vestbakken  
931 Volcanic Province can have suffered late steepening. Contraction expressed as fold  
932 systems with fold axes paralleling the basin margins development seems to  
933 correspond very well to the observed structural configuration of the Vestbakken  
934 Volcanic Province. Here pronounced tectonic inversion is focused along the N-S-  
935 striking basin margins and along some NE-SW-striking faults in the central parts  
936 of the basin. Pronounced shortening also occurred inside individual reactivated  
937 fault blocks either by bulging of the entire sedimentary sequence or as trains of  
938 folds (**Figure 12**).

939

940 The restraining bend configuration in the northern part of segment 2 was  
941 characterized by increasing contraction across strike-slip fault strands that  
942 splayed out to the northwest from the central part of segment 2 in an early stage  
943 of dextral shear. This deformation was terminated by the end of phase 1 by  
944 stacking of oblique contraction faults (PSE-5 and PSE-6-structures), defining an  
945 antiformal stack-like structure. This type of deformation falls outside the main  
946 area, but to the north this type of oblique shortening during the Eocene (phase 1)  
947 was accommodated by regional-scale strain partitioning (Leever et al., 2011a,b).

948

949 The Vestbakken Volcanic Province is characterized by extensive regional  
950 shortening. Onset of this event of inversion/contraction is dated to early Miocene  
951 (Jebsen & Faleide, 1998, Giennenas, 2018) and this deformation included two  
952 main structural fold styles. The first includes upright to steeply inclined closed to  
953 open anticlines that are typically present in the hanging wall of master faults.  
954 These folds typically have wavelengths in the order of 2.5 to 4.5 kilometers, and  
955 amplitudes of several hundred meters. Most commonly they appear with head-on  
956 snakehead-structures and are interpreted as buckle folds, albeit a component

957 shear may occur in the areas of the most intense deformation, giving a snake-head-  
958 type geometry. The second style includes gentle to open anticline-syncline pairs  
959 with upright or steep to inclined axial planes with wavelengths in the order of 5  
960 to 7 kilometers and amplitudes of several tens of meters to several hundred  
961 meters. We associate those with the PSE-4-type structures as defined in the  
962 BarMar-experiments. These folds are situated in positions where sedimentary  
963 sequences have been pushed against buttresses provided by master faults along  
964 the basin margins. The PSE-6 folds developed as fold trains in the interior basins,  
965 where buttressing against larger fault walls was uncommon. Also, this pattern fits  
966 well with the development and geometry seen in the BarMar-experiments, where  
967 folding started in the central parts of the closing basins before folding of the  
968 marginal parts of the basin. In the closing stage the folding and inversion of master  
969 faults remained focused along the basin margins.

970

971 The experiments clearly demonstrated that contraction by buckle folding was the  
972 main shortening mechanism of the margin-parallel basin system generated in  
973 phase 2 (orthogonal or oblique extension) in all segments. In the Vestbakken  
974 Volcanic Province segments of the Knølegga Fault Zone, the EBF and the major  
975 intra-basinal faults contain clear evidence for tectonic inversion, whereas this is  
976 less pronounced in others. The hanging wall of the EBF is partly affected by fish-  
977 hook-type inversion anticlines (Ramsey & Huber, 1987; Griera et al., 2018)  
978 (**Figure 2D, E**), or isolated hanging wall anticlines or pairs or trains of synclines  
979 and anticlines (e.g., Roberts, 1989; Coward et al., 1991; Cartwright, 1989; Mitra,  
980 1993; Uliana et al., 1995; Beauchamp et al. 1996; Gabrielsen et al. 1997; Henk &  
981 Nemcok 2008), the fold style and associated faults probably being influenced by  
982 the orientation and steepness of the pre-inversion fault (Williams et al., 1989;  
983 Cooper et al., 1989; Cooper & Warren, 2010). Some structures of this type can still  
984 be followed for many kilometers having consistent geometry and attitude. These  
985 structures have not been much modified by reactivation and are invariably found  
986 in the proximal parts footwalls of master faults, suggesting that these are  
987 inversion structures that correlate to PSE-type 5-structures in the experiments  
988 developed in areas of focused contraction along pre-existing fault scarps during  
989 Miocene inversion.

990

991 Trains of folds with smaller amplitudes and higher frequency are sometimes  
992 found in fault blocks in the central part of the Vestbakken Volcanic Province  
993 (**Figure 12F**). Although these structures are not dateable by seismic  
994 stratigraphical methods (onlap configurations etc.) we regard these fold strains to  
995 be correlatable with the tight folds generated in the inversion stage in the  
996 experiments (PSE-6-structures) and that they are contemporaneous with the PSE-  
997 5-structures.

998

999 Segment 1 in the experiments, which corresponds to the Senja Shear Margin  
1000 segment, displays a structural pattern that is a hybrid between segments 1 and 2.  
1001 It contains incipient structural elements that were developed in full in segments 2  
1002 and 3, segment 2 being dominated by releasing and restraining bend  
1003 configurations and segment 3 dominated by neutral shear. Due to internal  
1004 configurations, the three segments were affected to secondary (oblique) opening  
1005 and contraction in various fashions. Understanding these differences was much  
1006 promoted by the comparison of seismic and model data.

1007

## 1008 **Summary and conclusions**

1009

1010 The Barents Shear Margin is a challenging target for structural analysis both  
1011 because it represents a geometrically complex structural system with a multistage  
1012 history, but also because high-quality (3D) seismic reflection data are limited and  
1013 many structures and sedimentary systems generated in the earlier tectono-  
1014 thermal stages have been overprinted and obliterated by younger events. This  
1015 makes analogue experiments very useful in the analysis, since they offer a  
1016 template for what kind of structural elements can be expected. By constraining the  
1017 experimental model according to the outline of the margin geometry and imposing  
1018 a dynamic stress model in harmony according to the state-of-the-art knowledge  
1019 about the regional tectono-sedimentological development, we were able to  
1020 interpret the observations done in seismic reflection data in a new light.

1021

1022 Our observations confirmed that the main segments of the Barents Shear Margin,  
1023 albeit undergoing the same regional stress regime, display contrasting structural  
1024 configurations. The deformation in segment 2 in the BarMar-experiments, was  
1025 determined by releasing and restraining bends in the southern and northern  
1026 parts, respectively. Thus, the southern part, corresponding to the Vestbakken  
1027 Volcanic Province, was dominated by the development of a regional-scale  
1028 extensional shear duplex. By continued shear the basin developed into a full-  
1029 fledged pull-apart basin or rhomb graben in which rotating fault blocks were  
1030 trapped. The pull-apart basin became the nucleus for greater basin systems to  
1031 develop in the following phase of extension also providing the space for folds to  
1032 develop in the contractional phase.

1033

1034 We conclude that fault- and fold systems found in the realm of the Vestbakken  
1035 Volcanic Province are in accordance with a three-stage development that includes  
1036 dextral shear followed by oblique extension and contraction ( $325/145^0$ ) along a  
1037 shear margin with composite geometry. Folds with NE-SW-trending fold axes are  
1038 dominant in wider area of the Vestbakken Volcanic Province and are dominated  
1039 by folds in the hanging walls of (older) normal faults, sometimes characterized by  
1040 narrow, snakehead- or harpoon-type structures that are typical for tectonic  
1041 inversion.

1042

1043 Comparing seismic mapping and analogue experiments it is evident that a main  
1044 challenge in analyzing the structural pattern in shear margins of complex  
1045 geometry and multiple reactivation is the low potential for preservation of  
1046 structures that were generated in the earliest stages of the development.

1047

1048

1049

1050

1051

1052

1053

1054

1055 **Author contribution**

1056 R.H. Gabrielsen: Contributions to outline, design and performance of experiments.  
1057 First writing and revisions of manuscript. First drafts of figures.

1058 P.A. Giennenas: Seismic interpretation in the Vestbakken Volcanic Province.  
1059 Identification and description of fold families.

1060 D. Sokoutis: Main responsibility for set-up, performance and handling of  
1061 experiments. Revisions of manuscript.

1062 E. Willigshofer: Performance and handling of experiments. Revisions of  
1063 manuscript. Design and revisions of figure material.

1064 M. Hassaan: Background seismic interpretation. Discussions and revisions of  
1065 manuscript. Design and revisions of figure material.

1066 J.I. Faleide: Regional interpretations and design of experiments. Participation in  
1067 performance and interpretations of experiments. Revisions of manuscript, design  
1068 and revisions of figure material.

1069

1070

1071 **Acknowledgements**

1072 The work was supported by ARCEX (Research Centre for Arctic Petroleum  
1073 Exploration), which was funded by the Research Council of Norway (grant number  
1074 228107) together with 10 academic and six industry (Equinor, Vår Energi, Aker  
1075 BP, Lundin Energy Norway, OMV and Wintershall Dea) partners. Muhammad  
1076 Hassaan was funded by the Suprabasins project (Research Council of Norway  
1077 grant no. 295208). We thank to Schlumberger for providing us with academic  
1078 licenses for Petrel software to do seismic interpretation. Two anonymous  
1079 reviewers and the editors of this special volume provided comments, suggestions  
1080 and advice that enhanced the clarity and scientific quality of the paper.

1081

1082 **References**

1083

1084 Allemand, P. and Brun, J. P.: Width of continental rifts and rheological layering of the  
1085 lithosphere. *Tectonophysics*, 188, 63-69, 1991.

1086 Allmendinger, R. W.: Inverse and forward numerical modeling of threeshear fault-  
1087 propagation folds, *Tectonics*, 17(4), 640-656, 1998.

1088 Auzemery, A., Willingshofer, E., Sokoutis, D., Brun, J.- P., and Cloetingh, S. A. P. L.:  
1089 Passive margin inversion controlled by stability of the mantle lithosphere,  
1090 *Tectonophysics*, 817, 229042, 1-17, <https://doi.org/10.1016/j.tecto.2021.229042>, 2021.

1091 Aydin, A. and Nur, A.: Evolution of pull-apart basins and their scale independence.  
1092 *Tectonics*, 1, 91-105, 1982.

1093

1094 Ballard, J.-F., Brun, J.-P., and Van Ven Driessche, J.: Propagation des chevauchements  
1095 au-dessus des zones de décollement: modèles expérimentaux. *Comptes Rendus de*  
1096 *l'Académie des Sciences, Paris*, 11, 305, 1249-1253, 1987.

1097

1098 Basile, C.: Transform continental margins – Part 1: Concepts and models.  
1099 *Tectonophysics*, 661, pp.1-10. doi: 10.1016/j.tecto.2015.08.034, 2015.

1100

1101 Basile, C. and Brun, J.-P.: Transtensional faulting patterns ranging from pull-apart  
1102 basins to transform continental margins: an experimental investigation, *Journal of*  
1103 *Structural Geology*, 21,23-37, 1997.

1104

1105 Beauchamp, W., Barazangi, M., Demnati, A., and El Alji, M.: Intracontinental rifting  
1106 and inversion: Missouri Basin and Atlas Mountains, Morocco. *American Association of*  
1107 *Petroleum Geologists Bulletin*, 80(9), 1455-1482, 1996.

1108

1109 Bergh, S. G., Braathen, A., and Andresen, A.: Interaction of basement-involved and  
1110 thin-skinned tectonism in the Tertiary fold-and-thrust belt of Central Spitsbergen,  
1111 Svalbard. *American Association of Petroleum Geologists Bulletin*, 81(4), 637-661,  
1112 1997.

1113

1114 Bergh, S. G. and Grogan, P.: Tertiary structure of the Sørkapp-Hornsund Region, South  
1115 Spitsbergen, and implications for the offshore southern extension of the fold-thrust-  
1116 belt. *Norwegian Journal of Geology*, 83, 43-60, 2003.

1117

1118 Biddle, K. T. and Christie-Blick, N., (eds.): *Strike-Slip Deformation, Basin Formation,*  
1119 *and Sedimentation: Society of Economic Paleontologists and Mineralogists Special*  
1120 *Publication*, 37, 386 pp, 1985a.

1121

1122 Biddle, K. T. and Christie-Blick, N.: Glossary — Strike-slip deformation, basin  
1123 formation, and sedimentation, *in*: Biddle, K. T. and Christie-Blick, N. (eds.): *Strike-*  
1124 *Slip Deformation, Basin Formation, and Sedimentation: Society of Economic*  
1125 *Paleontologists and Mineralogists Special Publication*, 37, 375-386, 1985b.

1126

1127 Blaich, O. A., Tsikalas, F., and Faleide, J. I.: New insights into the tectono-stratigraphic  
1128 evolution of the southern Stappen High and the transition to Bjørnøya Basin, SW  
1129 Barents Sea, *Marine and Petroleum Geology*, 85, 89-105, doi:



- 1130 10.1016/j.marpetgeo.2017.04.015, 2017.  
1131  
1132 Breivik, A. J., Faleide, J. I., and Gudlaugsson, S. T.: Southwestern Barents Sea margin:  
1133 late Mesozoic sedimentary basins and crustal extension, *Tectonophysics*, 293, 21-44,  
1134 1998.  
1135  
1136 Breivik, A. J., Mjelde, R., Grogan, P., Shinamura, H., Murai, Y., and Nishimura, Y.:  
1137 Crustal structure and transform margin development south of Svalbard based on ocean  
1138 bottom seismometer data. *Tectonophysics*, 369, 37-70, 2003.
- 1139 Brekke, H.: The tectonic evolution of the Norwegian Sea continen- tal margin with  
1140 emphasis on the Vøring and Møre basins: Geological Society, London, Special  
1141 Publication, 136, 327–378, 2000.
- 1142 Brekke, H. and Riis, F.: Mesozoic tectonics and basin evolution of the Norwegian Shelf  
1143 between 60°N and 72°N. *Norsk Geologisk Tidsskrift*, 67, 295-322, 1987.  
1144  
1145 Burchfiel, B. C. and Stewart, J. H.: "Pull-apart" origin of the central segment of Death  
1146 Valley, California. *Geological Society of America Bulletin.*, 77, 439-442, 1966.  
1147  
1148 Campbell, J. D.: *En échelon* folding, *Economical Geology*, 53(4), 448-472, 1958.  
1149  
1150 Cartwright, J. A.: The kinematics of inversion in the Danish Central Graben. in:  
1151 M.A.Cooper & G.D.Williams (eds.): *Inversion Tectonics*. Geological Society of  
1152 London Special Publication, 44, 153-175, 1989.  
1153  
1154 Casas, A. M., Gapals, D., Nalpas, T., Besnard, K., and Román-Berdiel, T.: Analogue  
1155 models of transpressive systems, *Jornal of Structural Geology*, 23,733-743, 2001.  
1156  
1157 Christie-Blick, N. and Biddle, K. T.: Deformation and basin formation along strike-slip  
1158 faults. in: Biddle,K.T. & Christie-Blick,N. (eds.): *Strike-slip deformation, basin*  
1159 *formation and sedimentation*. Society of Economic Mineralogists and Palaeontologists  
1160 (Tulsa Oklahoma), Special Publication, 37, 1-34, 1985.  
1161  
1162 Cloos, H.: Experimenten zur inneren Tectonick, *Zentralblatt für Mineralogie, Geologie*  
1163 *und Palaentologie*, 1928B, 609-621, 1928.  
1164  
1165 Cloos, H.: Experimental analysis of fracture patterns, *Geological Society of America*  
1166 *Bulletin*, 66(3), 241-256, 1955.  
1167  
1168 Cooper, M. and Warren, M. J.: The geometric characteristics, genesis and petroleum  
1169 significance of inversion structures, in Law,R.D., Butler,R.W.H., Holdsworth,R.E.,  
1170 Krabbendam,M. & Strachan,R.A. (eds.): *Continental Tectonics and Mountain*  
1171 *Building: The Lagacy of Peache and Horne*, Geological Society of London, Special  
1172 *Publication*, 335, 827-846, 2010.  
1173  
1174 Cooper, M. A., Williams, G. D., de Graciansky, P. C., Murphy, R. W., Needham, T.,  
1175 de Paor, D., Stoneley, R., Todd, S. P., Turner, J. P., and Ziegler, P. A.: Inversion  
1176 tectonics – a discussion. Geological Society, London, Special Publications, 44, 335-  
1177 347, 1989.

1178  
1179 Coward, M.: Inversion tectonics, in: Hancock,P.L. (ed.): Continental Deformation,  
1180 Pergamon Press, 289-304, 1994.  
1181  
1182 Coward, M. P., Gillcrist, R., and Trudgill, B.: Extensional structures and their tectonic  
1183 inversion in the Western Alps, *in*: A.M.Roberts, G.Yielding & B.Freeman (eds.): The  
1184 Geometry of Normal Faults. Geological Society of London Special Publication, 56, 93-  
1185 112, 1991.  
1186  
1187 Crowell, J.: Displacement along the San Andreas Fault, California, Geological Society  
1188 of America Special Papers, 71, 59pp, 1962.  
1189  
1190 Crowell, J. C.: Origin of late Cenozoic basins in southern California. in R.H.Dorr &  
1191 R.H.Shaver (eds.): Modern and ancient geosynclinal sedimentation. SEPM Special  
1192 Publication, 19, 292-303, 1974a.  
1193  
1194 Crowell, J. C.: Implications of crustal stretching and shortening of coastal Ventura  
1195 Basin, in: Howell,D.G. (ed.): Aspects of the geological history of the California  
1196 continental Borderland, American Association of Petroleum Geologists, Pacific  
1197 Section, Publication 24, 365-382, 1974b.  
1198  
1199 Cunningham, W. D. and Mann,P. (eds.), 2007a: Tectonics of Strike-Slip Restraining  
1200 and Releasing Bends, Geological Society London Special Publication, 290, 482pp.  
1201  
1202 Cunningham, W. D. and Mann, P.: Tectonics of Strike-Slip Restraining and Releasing  
1203 Bends, *in*: Cunningham,W.D. & Mann,P. (eds.), 2007: Tectonics of Strike-Slip  
1204 Restraining and Releasing Bends, Geological Society London Special Publication, 290,  
1205 1-12, 2007b.  
1206  
1207 Dauteuil, O. and Mart, Y.: Analogue modeling of faulting pattern, ductile deformation,  
1208 and vertical motion in strike-slip fault zones, *Tectonics*, 17(2), 303-310, 1998.  
1209  
1210 Del Ventisette, C., Montanari, D., Sani, F., Bonini, M., and Corti, G.: Reply to comment  
1211 by J. Wickham on “Basin inversion and fault reactivation in laboratory  
1212 experiments”. *Journal of Structural Geology* 29, 1417–1418, 2007.  
1213  
1214 Dooley, T. and McClay, K.: Analog modeling of pull-apart basins, *American*  
1215 *Association of Petroleum Geologists Bulletin*, 81(11), 1804-1826, 1997.  
1216  
1217 Dooley, T. P. and Schreurs, G.: Analogue modelling of intraplate strike-slip tectonics:  
1218 A review and new experimental results, *Tectonophysics*, 574-575, 1-71, 2012.  
1219  
1220 Doré, A. G. and Lundin, E. R.: Cenozoic compressional structures on the NE Atlantic  
1221 margin: nature, origin and potential significance for hydrocarbon exploration.  
1222 *Petroleum Geosciences*, 2, 299-311, 1996.  
1223  
1224 Doré, A. G., Lundin, E. R., Gibbons, A., Sømme, T. O., and Tørudbakken, B. O.:  
1225 Transform margins of the Arctic: a synthesis and re-evaluation *in*: Nemcok,M.,  
1226 Rybár,S., Sinha,S.T., Hermeston,S.A. & Ledvényiová,L. (eds.): Transform Margins,:

1227 Development, Control and Petroleum Systems, Geological Society London, Special  
1228 Publication, 431, 63-94, 2016.  
1229  
1230 Doré, A. G., Lundin, E. R., Jensen, L. N., Birkeland, Ø., Eliassen, P. E., and Fichler,  
1231 C.: Principal tectonic events in the evolution of the northwest European Atlantic  
1232 margin. In: A.J.Fleet & S.A.R.Boldy (eds.): Petroleum Geology of Northwest Europe:  
1233 Proceedings of the Fifth Conference (Geological Society of London), 41-61, 1999.  
1234  
1235 Eidvin, T., Goll, R. M., Grogan, P., Smelror, M., and Ulleberg, K.: The Pleistocene to  
1236 Middle Eocene stratigraphy and geological evolution of the western Barents Sea  
1237 continental margin ta well site 731675-1 (Bjørnøya West area). Norsk Geologisk  
1238 Tidsskrift, 78, 99-123, 1998.  
1239  
1240 Eidvin, T., Jansen, E., and Riis, F.: Chronology of Tertiary fan deposits off the western  
1241 Barents Sea: Implications for the uplift and erosion history of the Barents Shelf. Marine  
1242 Geology, 112, 109-131, 1993.  
1243  
1244 Eldholm, O., Faleide, J.I. & Myhre, A.M., 1987: Continent-ocean transition at the  
1245 western Barents Sea/Svalbard continental margin. Geology, 15, 1118-1122.  
1246  
1247 Eldholm, O., Thiede, J., and Taylor, E.: Evolution of the Vøring volcanic margin, *in*:  
1248 Eldholm, O., Thiede, J., and Taylor, E., (eds.): Proceedings of the Ocean Drilling  
1249 Program, Scientific Results, 104: College Station (Ocean Drilling Program), TX, 1033–  
1250 1065, 1989.  
1251  
1252 Eldholm, O., Tsikalas, F., and Faleide, J. I.: Continental margin off Norway 62-  
1253 75°N: Paleogene tectono-magmatic segmentation and sedimentation. Geological  
1254 Society of London Special Publication, 197, 39-68, 2002.  
1255  
1256 Emmons, R. C.: Strike-slip rupture patterns in sand models, Tectonophysics, 7, 71-87,  
1257 1969.  
1258  
1259 Faugère, E., Brun, J.-P., and Van Den Driessche, J.: Bassins asymétriques en  
1260 extension pure et en détachements: Modèles expérimentaux, Bulletin Centre Recherche  
1261 Exploration et Production Elf Aquitaine, 10(2), 13-21, 1986.  
1262  
1263 Faleide, J. I., Bjørlykke, K., and Gabrielsen, R. H.: Geology of the Norwegian Shelf.  
1264 *in*: Bjørlykke, K.: Petroleum Geoscience: From Sedimentary Environments to Rock  
1265 Physics 2<sup>nd</sup> Edition, Springer-Verlag, Berlin Heidelberg, Chapter 25, 603 -637, 2015.  
1266  
1267 Faleide, J. I., Myhre, A. M., and Eldholm, O.: Early Tertiary volcanism at the western  
1268 Barents Sea margin. in: A.C.Morton & L.M.Parsons (eds.): Early Tertiary volcanism  
1269 and the opening of the NE Atlantic. Geological Society of London Special Publication,  
1270 39, 135-146, 1988.  
1271  
1272 Faleide, J. I., Tsikalas, F., Breivik, A. J, Mjelde, R., Ritzmann, O., Engen, Ø., Wilson,  
1273 J., and Eldholm, O.: Structure and evolution of the continental margin off Norway and  
1274 the Barents Sea. Episodes, 31(1), 82-91, 2008.  
1275

- 1276 Faleide, J. I., Vågnes, E., and Gudlaugsson, S. T.: Late Mesozoic - Cenozoic evolution  
1277 of the south-western Barents Sea in a regional rift-shear tectonic setting. *Marine and*  
1278 *Petroleum Geology*, 10, 186-214, 1993.
- 1279  
1280 Fichler, C. and Pastore, Z.: Petrology and crystalline crust in the southwestern Barents  
1281 Sea inferred from geophysical data. *Norwegian Journal of Geology*, 102, 41pp,  
1282 <https://dx.doi.org/10.17850/njg102-2-2, 2022>.
- 1283  
1284 Freund, R.: The Hope Fault, a strike-slip fault in New Zealand, *New Zealand*  
1285 *Geological Survey Bulletin*, 86, 1-49, 1971.
- 1286  
1287 Gabrielsen, R. H.: Structural elements in graben systems and their influence on  
1288 hydrocarbon trap types. in: A.M. Spencer (ed.): *Habitat of Hydrocarbons on the*  
1289 *Norwegian Continental Shelf*. *Norw. Petrol. Soc. (Graham & Trotman)*, 55 – 60, 1986.
- 1290  
1291 Gabrielsen, R. H., Færseth, R. B., Jensen, L. N., Kalheim, J. E., and Riis, F.: Structural  
1292 elements of the Norwegian Continental Shelf. Part I: The Barents Sea Region.  
1293 *Norwegian Petroleum Directorate, Bulletin*, 6, 33pp, 1990.
- 1294  
1295 Gabrielsen, R. H., Grunnaleite, I., and Rasmussen, E.: Cretaceous and Tertiary  
1296 inversion in the Bjørnøyrenna Fault Complex, south-western Barents Sea. *Marine and*  
1297 *Petroleum Geology*, 142, 165-178, 1997.
- 1298  
1299 Gac, S., Klitzke, P., Minakov, A., Faleide, J. I., and Scheck-Wenderoth, M.:  
1300 Lithospheric strength and elastic thickness of the Barents Sea and Kara Sea region,  
1301 *Tectonophysics*, 691, 120-132, doi: 10.106/j.tecto.2016.04.028, 2016.
- 1302  
1303 Gaina, C., Gernigon, L., and Ball, P.: Palaeocene – Recent plate boundaries in the NE  
1304 Atlantic and the formation of the Jan Mayen microcontinent. *Journal of the Geological*  
1305 *Society, London*, 166(4), 601-616, 2009.
- 1306  
1307 Ganerød, M., Smethurst, M. A., Torsvik, T. H., Prestvik, T., Rouse, S., McKenna, C.,  
1308 van Hinsbergen, D.J.J., and Hendriks, W. W. H.: The North Atlantic Igneous Province  
1309 reconstructed and its relation to the Plume Generation Zone: the Antrim Lava Group  
1310 revisited. *Geophysical Journal International*, 182, 183-202, doi: 10.1111/j.1365-  
246X.2010.04620.x, 2010.
- 1311  
1312 Giennenas, P. A.: The Structural Development of the Vestbakken Volcanic Province,  
1313 Western Barents Sea. Relation between Faults and Folds, Unpubl. Master thesis,  
1314 University of Oslo, 89 pp, 2018.
- 1315  
1316 Graymer, R. W., Langenheim, V. E., Simpson, R. W., Jachens, R. C., and Ponce, D.  
1317 A.: Relative simple through-going fault planes at large-earthquake depth may be  
1318 concealed by surface complexity of strike-slip faults, *in*: Cunningham, W.D. & Mann, P.  
1319 (eds.): *Tectonics of Strike-Slip Restraining and Releasing Bends*, Geological Society  
1320 London Special Publication, 290, 189-201, 2007.
- 1321  
1322 Griera, A., Gomez Rivas, E., and Llorens, M.- G.: The influence of layer-interface  
1323 geometry of single-layer folding. *Geological Society of London Special Publication*  
487, SP487:4, 2018.

- 1324  
1325 Grogan, P., Østvedt-Ghazi, A.- M., Larssen, G. B., Fotland, B., Nyberg, K., Dahlgren,  
1326 S., and Eidvin, T.: Structural elements and petroleum geology of the Norwegian sector  
1327 of the northern Barents sea. *in: Fleet, A.J. & Boldry, S.A.R. (eds.): Petroleum Geology*  
1328 *of Northwest Europe: Proceedings of the 5th Conference, Geological Society of*  
1329 *London, 247-259, 1999.*  
1330  
1331 Groshong, R. H.: Half-graben structures: balanced models of extensional fault bend  
1332 folds, *Geological Society of America Bulletin*, 101, 96-195, 1989.  
1333  
1334 Gudlaugsson, S. T. and Faleide, J. I.: The continental margin between Spitsbergen &  
1335 Bjørnøya, *in: O.Eiken (ed.): Seismic Atlas of Western Svalbard, Norsk Polarinstitutt*  
1336 *Meddelelser*, 130, 11-13, 1994.  
1337  
1338 Gudlaugsson, S. T., Faleide, J. I., Johansen, S. E., and Breivik, A. J.: Late Palaeozoic  
1339 structural development of the south-western Barents Sea. *Marine and Petroleum*  
1340 *Geology*, 15, 73-102, 1998.  
1341  
1342 Hamblin, W. K.: Origin of "reverse drag" on the down-thrown side of normal faults,  
1343 *Geological Society of America Bulletin*, 76, 1145-1164, 1965.  
1344  
1345 Hanisch, J.: The Cretaceous opening of the Northeast Atlantic. *Tectonophysics*, 101, 1-  
1346 23, 1984.  
1347  
1348 Harding, T. P.: Petroleum traps associated with wrench faults. *American Association*  
1349 *of Petroleum Geologists Bulletin*, 58, 1290-1304, 1974.  
1350  
1351 Harding, T. P. and Lowell, J. D.: Structural styles, their plate tectonic habitats, and  
1352 hydrocarbon traps in petroleum provinces, *American Association of Petroleum*  
1353 *Geologists Bulletin*, 63, 1016-1058, 1979.  
1354  
1355 Harland, W. B.: The tectonic evolution of the Arctic-North Atlantic Region, *in:*  
1356 *Taylor, J.H., Rutten, M.G., Hales, A.L., Shackelton, R.M., Nairn, A.E. & Harland: W.B.:*  
1357 *Discussion, A Symposium on Continental Drift, Philosophical Transactions of the*  
1358 *Royal Society of London, Series A, 258, 1088, 59-75, 1965.*  
1359  
1360 Harland, W. B.: Contributions of Spitsbergen to understanding of tectonic evolution of  
1361 North Atlantic Region, *American Association of Petroleum Geologists, Memoir 12,*  
1362 *817-851, 1969.*  
1363  
1364 Harland, W. B.: Tectonic transpression in Caledonian Spitsbergen, *Geological*  
1365 *Magazine*, 108, 27-42, 1971.  
1366  
1367 Henk, A. and Nemcok, M.: Stress and fracture prediction in inverted half-graben  
1368 structures. *Journal of Structural Geology*, 30(1), 81-97, 2008.
- 1369 Horni, J. Á., Hopper, J. R., Blischke, A., Geisler, W. H., Stewart, M., Mcdermott, K.,  
1370 Judge, M., Erlendsson, Ö, and Ártung, U. E.: Regional Distribution of Volcanism within  
1371 the North Atlantic Igneous Province. *The NE Atlantic Region: A Reappraisal of*  
1372 *Crustal Structure, Tectonostratigraphy and Magmatic Evolution. Geological*



- 1373 Society, London, Special Publications, 447, 105–125,  
1374 <https://doi.org/10.1144/SP447.18>, 2017.
- 1375 Horsfield, W. T.: An experimental approach to basement-controlled faulting.  
1376 *Geologie en Mijnbouw*, 56(4), 3634-370, 1977.  
1377
- 1378 Hubbert, M. K.: Theory of scale models as applied to the study of geologic  
1379 structures, *Bulletin Geological Society of America*, 48, 1459-1520, 1937.
- 1380 Jebsen, C. and Faleide, J. I.: Tertiary rifting and magmatism at the western Barents Sea  
1381 margin (Vestbakken volcanic province). III international conference on Arctic margins,  
1382 ICAM III; abstracts; plenary lectures, talks and posters, 92, 1998.
- 1383 Khalil, S. M. and McClay, K. R.: 3D geometry and kinematic evolution of extensional  
1384 fault-related folds, NW Red Sea, Egypt. in: Childs, C., Holdsworth, R. E., Jackson, C. A. L.,  
1385 Manzocchi, T., Walsh, J. J. & Yielding, G. (eds.): *The Geometry and Growth of Normal  
1386 Faults*, Geological Society, London, Special Publication 439,  
1387 [doi.org/10.1144/SP439.11](https://doi.org/10.1144/SP439.11), 2016.  
1388
- 1389 Klinkmüller, M., Schreurs, G., Rosenau, M., and Kemnitz, H.: Properties of  
1390 granular analogue model materials: a community wide survey. *Tectonophysics*  
1391 684, 23–38. <http://dx.doi.org/10.1016/j.tecto.2016.01.017>.feb., 2016.  
1392
- 1393 Knutsen, S.-M. and Larsen, K. I.: The late Mesozoic and Cenozoic evolution of the  
1394 Sørvestsnaget Basin: A tectonostratigraphic mirror for regional events along the  
1395 Southwestern Barents Sea Margin? *Marine and Petroleum Geology*, 14(1), 27-54,  
1396 1997.  
1397
- 1398 Kristensen, T. B., Rotevatn, A., Marvik, M., Henstra, G. A., Gawthorpe, R. L. and  
1399 Ravnås, R.: Structural evolution of sheared basin margins: the role of strain  
1400 partitioning. *Sørvestsnaget Basin, Norwegian Barents Sea, Basin Research*, (2017),  
1401 1-23, [doi:10.1111/bre.12235](https://doi.org/10.1111/bre.12235), 2017.  
1402
- 1403 Le Calvez, J.-H. and Vendeville, B. C.: Experimental designs to mode along strike-  
1404 slip fault interaction. *in*: Scellart, W. P. & Passchier, C. (eds.). *Analogue Modeling of  
1405 large-scale Tectonic Processes*, *Journal of Virtual Explorer*, 7, 7-23, 2002.  
1406
- 1407 Leever, K. A., Gabrielsen, R. H., Sokoutis, D. and Willingshofer, E.: The effect of  
1408 convergence angle on the kinematic evolution of strain partitioning in  
1409 transpressional brittle wedges: insight from analog modeling and high resolution  
1410 digital image analysis. *Tectonics*, 30, TC2013, 1-25, [doi: 10.1029/2009TC002649](https://doi.org/10.1029/2009TC002649),  
1411 2011a.  
1412
- 1413 Leever, K. A., Gabrielsen, R. H., Faleide, J. I. and Braathen, A.: A transpressional  
1414 origin for the West Spitsbergen Fold and Thrust Belt - insight from analog  
1415 modeling. *Tectonics*, 30, TC2014, 1- 24, [doi: 10.1029/2010TC002753](https://doi.org/10.1029/2010TC002753), 2011b.  
1416
- 1417 Libak, A., Mjelde, R., Keers, H., Faleide, J. I. and Murai, Y.: An intergrated  
1418 geophysical study of Vestbakken Volcanic Province, western Barents Sea

- 1419 continental margin, and adjacent oceanic crust, *Marine Geophysical Research*,  
1420 33(2), 187-207, 2012a.  
1421
- 1422 Libak, A., Eide, C. H., Mjelde, R., Keers, H., and Flüh, E. R.: From pull-apart basins to  
1423 ultraslow spreading: Results from the western Barents Sea Margin.  
1424 *Tectonophysics*, 514–517, 44–61, 2012b.  
1425
- 1426 Lorenzo, J. M.: Sheared continental margins: an overview, *Geo-Marine Letters*,  
1427 17(1), 1-3, 1997.
- 1428 Lowell, J. D.: Spitsbergen Tertiary orogenic belt and the Spitsbergen fracture zone,  
1429 *Geol. Soc. Am. Bull.*, 83, 3091–3102, doi:10.1130/0016-  
1430 7606(1972)83[3091:STOBAT]2.0.CO;2, 1972.
- 1431 Lundin, E. R. and Doré, A. G.: A tectonic model for the Norwegian passive margin  
1432 with implications for the NE Atlantic.: Early Cretaceous to break-up. *Journal of the*  
1433 *Geological Society London*, 154, 545-550, 1997.  
1434
- 1435 Lundin, E. R., Doré, A. G., Rønning, K. and Kyrkjebø, R.: Repeated inversion in the  
1436 Late Cretaceous-Cenozoic northern Vøring Basin, offshore Norway, *Petroleum*  
1437 *Geoscience*, 19(4), 329-341, 2013.  
1438
- 1439 Luth, S., Willingshofer, E., Sokoutis, D. and Cloetingh, S.: Analogue modelling of  
1440 continental collision: Influence of plate coupling on mantle lithosphere subduction,  
1441 crustal deformation and surface topography, *Tectonophysics*, 4184, 87-102, doi:  
1442 10.1016/j.tecto2009.08.043, 2010.
- 1443 Maher, H. D., Jr., Bergh, S., Braathen, A., and Ohta, Y.: Svartfjella, Eidembukta, and  
1444 Daudmannsodden lineament: Tertiary orogen-parallel motion in the crystalline  
1445 hinterland of Spitsbergen's fold-thrust belt, *Tectonics*, 16(1), 88–106,  
1446 doi:10.1029/96TC02616, 1997.
- 1447 Mandl, G., de Jong, L. N. J., and Maltha, A.: Shear zones in granular material. *Rock*  
1448 *Mechanics*, 9, 95–144, 1977.  
1449
- 1450 Manduit, T. and Dauteuil, O.: Small scale modeling of oceanic transform zones,  
1451 *Journal of Geophysical Research*, 101(B9), 20195-20209, 1996.  
1452
- 1453 Mann, P.: Global catalogue, classification and tectonic origins of restraining and  
1454 releasing bends on active and ancient strike-slip fault systems. *in*:  
1455 Cunningham, W.D. & Mann, P. (eds.), 2007: *Tectonics of Strike-Slip Restraining and*  
1456 *Releasing Bends*, Geological Society London Special Publication, 290, 13-142,  
1457 2007.  
1458
- 1459 Mann, P., Hempton, M. R., Bradley, D. C., and Burke, K.: Development of pull-apart  
1460 basins. *Journal of Geology*, 91(5), 529-554, 1983.  
1461
- 1462 Mascle, J. and Blarez, E.: Evidence for transform margin evolution from the Ivory  
1463 Coast Ghana continental margin, *Nature*, 326, 378-381, 1987.

1464  
1465 McClay, K. R.: Extensional fault systems in sedimentary basins. A review of  
1466 analogue model studies, *Marine and Petroleum Geology*, 7, 206-233, 1990.  
1467  
1468 Mitra, S.: Geometry and kinematic evolution of inversion structures. *American*  
1469 *Association of Petroleum Geologists Bulletin*, 77, 1159-1191, 1993.  
1470  
1471 Mitra, S. and Paul, D.: Structural geology and evolution of releasing and  
1472 restraining bends: Insights from laser-scanned experimental models,  
1473 *American Association of Petroleum Geologists Bulletin*, 95(7), 1147-1180, 2011.  
1474  
1475 Morgenstern, N. R. and Tchalenko, J. S.: Microscopic structures in kaolin subjected  
1476 to direct shear, *Géotechnique*, 17, 309-328, 1967.  
1477  
1478 Mosar, J., Torsvik, T. H., and the BAT Team: Opening of the Norwegian and  
1479 Greenland Seas: Plate tectonics in mid Norway since the late Permian. in: E.Eide  
1480 (ed.): *BATLAS. Mid Norwegian plate reconstruction atlas with global and Atlantic*  
1481 *perspectives. Geological Survey of Norway*, 48-59, 2002.  
1482  
1483 Mouslopoulou, V., Nicol, A., Little, T. A., and Walsh, J. J.: Terminations of large-  
1484 strike-slip faults: an alternative model from New Zealand, in: Cunningham, W.D. &  
1485 Mann, P. (eds.): *Tectonics of Strike-Slip Restraining and Releasing Bends*,  
1486 *Geological Society London Special Publication*, 290, 387- 415, 2007.  
1487  
1488 Mouslopoulou, V., Nicol, A., Walsh, J. J., Beetham, D., and Stagpoole, V.: Quaternary  
1489 temporal stability of a regional strike-slip and rift fault interaction. *Journal of*  
1490 *Structural Geology*, 30, 451-463, 2008.  
1491  
1492 Myhre, A. M. and Eldholm, O.: The western Svalbard margin (74-80°N). *Marine and*  
1493 *Petroleum Geology*, 5, 134-156, 1988.  
1494  
1495 Myhre, A. M., Eldholm, O., and Sundvor, E.: The margin between Senja and  
1496 Spitsbergen Fracture Zones: Implications from plate tectonics. *Tectonophysics*,  
1497 89, 33-50, 1982.  
1498  
1499 Naylor, M. A., Mandl, G., and Sijpestijn, C. H. K.: Fault geometries in basement-  
1500 induced wrench faulting under different initial stress states. *Journal of Structural*  
1501 *Geology*, 8, 737-752, 1986.  
1502  
1503 Nemcok, M., Rybár, S., Sinha, S. T., Hermeston, S. A., and Ledvényiová, L.:  
1504 Transform margins: development, controls and petroleum systems – an  
1505 introduction. in: Nemcok, M., Rybár, S., Sinha, S.T., Hermeston, S.A. & Ledvényiová, L.  
1506 (eds.): *Transform Margins: Development, Control and Petroleum Systems*,  
1507 *Geological Society London, Special Publication*, 431, 1-38, 2016.  
1508  
1509 Odonne, F. and Vialon, P.: Analogue models of folds above a wrench fault,  
1510 *Tectonophysics*, 99, 31-46, 1983.  
1511

1512 Pace, P. and Calamita, F.: Push-up inversion structures v. fault-bend reactivation  
1513 anticlines along oblique thrust ramps: examples from the Apennines fold-and-  
1514 thrust-belt, Italy, *Journal Geological Society London*, 171, 227-238, 2014.  
1515  
1516 Pascal, C. and Gabrielsen, R. H.: Numerical modelling of Cenozoic stress patterns  
1517 in the mid Norwegian Margin and the northern North Sea. *Tectonics*, 20(4), 585-  
1518 599, 2001.  
1519  
1520 Pascal, C., Roberts, D., and Gabrielsen, R. H.: Quantification of neotectonic stress  
1521 orientations and magnitudes from field observations in Finnmark, northern  
1522 Norway. *Journal of Structural Geology*, 27, 859-870, 2005.  
1523  
1524 Peacock, D. C. P., Nixon, C. W., Rotevatn, A., Sanderson, D. J., and Zuluaga, L. F.:  
1525 Glossary of fault and other fracture networks, *Journal of Structural Geology*, 92,  
1526 12-29, doi: 10.1016/j.jgs2016.09.008, 2016.  
1527  
1528 Perez-Garcia, C., Safranova, P. A., Mienert, J., Berndt, C., and Andreassen, K.:  
1529 Extensional rise and fall of a salt diapir in the Sørvestsnaget Basin, SW Barents Sea.  
1530 *Marine and Petroleum Geology*, 46, 129-134, 2013.  
1531  
1532 Planke, S., Alvestad, E., and Eldholm, O.: Seismic characteristics of  
1533 basaltic extrusive and intrusive rocks: The Leading Edge, 18(3), 342-348.  
1534 <https://doi-org.ezproxy.uio.no/10.1190/1.1438289>, 1999.  
1535  
1536 Ramberg, H.: Gravity, deformation and the Earth's crust, Academic Press, New  
1537 York, 214pp, 1967.  
1538  
1539 Ramberg, H.: Gravity, deformation and the Earth's crust, 2nd edition. Academic  
1540 Press, New York 452pp, 1981.  
1541  
1542 Ramsay, J. G. and Huber, M. I.: The techniques of modern structural geology. Vol.  
1543 2: Folds and fractures. Academic Press, London, 309-700, 1987.  
1544  
1545 Reemst, P., Cloetingh, S., and Fanavoll, S.: Tectonostratigraphic modelling of  
1546 Cenozoic uplift and erosion in the south-western Barents Sea. *Marine and  
1547 Petroleum Geology*, 11, 478-490, 1994.  
1548  
1549 Richard, P. D., Ballard, B., Colletta, B., and Cobbold, P. R.: Naissance et evolution de  
1550 failles au dessus d'un décrochement de socle: Modelisation experimental et  
1551 tomographie, *C. R. Acad.Sci. Paris*, 308,9, 2111-2118, 1989.  
1552  
1553 Richard, P. D. and Cobbold, P. R.: Structures et fleur positives et décrochements  
1554 crustaux: mdélisation analogiuque et interpretation mecanique,  
1555 *C.R.Acad.Sci.Paris*, 308, 553-560, 1989.  
1556  
1557 Richard, P. and Krantz, R. W.: Experiments on fault reactivation in strike-slip  
1558 mode, *Tectonophysics*, 188, 117-131, 1991.  
1559

- 1560 Richard, P., Mocquet, B., and Cobbold, P. R.: Experiments on simultaneous faulting  
1561 and folding above a basement wrench fault, *Tectonophysics*, 188, 133-141, 1991.  
1562
- 1563 Riedel, W.: Zur Mechanik geologischer Brucherscheinungen. *Centralblatt für*  
1564 *Mineralogie, Geologie und Paläontologie*, 1929B, 354-368, 1929.  
1565
- 1566 Riis, F., Vollset, J., and Sand, M.: Tectonic development of the western margin of the  
1567 Barents Sea and adjacent areas. in: M.T.Halbouty (ed.): *Future petroleum*  
1568 *provinces of the World. American Association of Petroleum Geologists Memoir*,  
1569 40, 661-667, 1986.  
1570
- 1571 Roberts, D. G.: Basin inversion in and around the British Isles, in: M.A.Cooper &  
1572 G.D.Williams (eds.): *Inversion Tectonics. Geological Society of London Special*  
1573 *Publication*, 44, 131-150, 1989.  
1574
- 1575 Ryseth, A., Augustson, J. H., Charnock, M., Haugrud, O., Knutsen, S.-M., Midbøe, P.  
1576 S., Opsal, J. G. and Sundsbø, G.: Cenozoic stratigraphy and evolution of the  
1577 Sørvestsnaget Basin, southwestern Barents Sea. *Norwegian Journal of Geology*, 83,  
1578 107-130, 2003.
- 1579 Saunders, A. D., Fitton, J. G., Kerr, A. C., Norry, M. J., and Kent, R. W.: The North  
1580 Atlantic Igneous Province: *Geophysical Monograph 100, American Geophysical*  
1581 *Union*, pp. 45-93, 1997.
- 1582 Scheurs, G.: Experiments on strike-slip faulting and block rotation, *Geology*,  
1583 22,567-570, 1990.  
1584
- 1585 Schreurs, G.: Fault development and interaction in distributed strike-slip shear  
1586 zones: an experimental approach. in: Storti,F., Holdsworth,R.E. & Salvini,F. (eds):  
1587 *Intraplate Strike-slip Deformation Belts, Geological Society of London Special*  
1588 *Publication*, 210, 35-82, 2003.  
1589
- 1590 Schreurs, G., Colletta, B.: Analogue modelling of faulting in zones of continental  
1591 transpression and transtension. in: Holdsworth, R.E., Strachan, R.A., Dewey, J.F.  
1592 (eds.), *Continental Transpressional and Transtensional Tectonics, Geological*  
1593 *Society of London Special Publication*, London, 135, 59-79, 1998.  
1594
- 1595 Schreurs, G. and Colletta, B.: Analogue modelling of continental transpression and  
1596 transtension. in: Scellart,W.P. & Passchier,C. (eds.): *Analogue Modelling of Large-*  
1597 *scale Tectonic Processes. Journal of the Virtual Explorer*, 7, 103-114, 2003.  
1598
- 1599 Seiler, C., Fletcher, J. M., Quigley, M. C., Gleadow, A. J. and Kohn, B. P.: Neogene  
1600 structural evolution of the Sierra San Felipe, Baja California: evidence of proto-gulf  
1601 transtension in the Gulf Extensional Province? *Tectonophysics*, 488(1), 87-109,  
1602 2010.  
1603
- 1604 Sims, D., Ferrill, D. A., and Stamatakos, J. A.: Role of a brittle décollement in the  
1605 development of pull-apart basins : experimental results and natural examples.  
1606 *Journal of Structural Geology*, 21, 533-554, 1999.



- 1607  
1608 Sokoutis, D.: Finite strain effects in experimental mullions. *Journal of Structural*  
1609 *Geology*, 9, 233-249, 1987.
- 1610 Stearns, D. W.: Faulting and forced folding in the Rocky Mountains Foreland,  
1611 *Geological Society of America Memoir*, 151, 1-38, 1978.
- 1612  
1613 Sylvester, A. G. (ed): *Wrench Fault Tectonics*, Selected papers reprinted from the  
1614 *AAPG Bulletin* and other geological journals, American Association of Petroleum  
1615 Geologists Reprint Series 28,3 74pp, 1985.
- 1616  
1617 Sylvester, A. G.: Strike-slip faults. *Geological Society of America Bulletin*, 100,  
1618 1666-1703, 1988.
- 1619  
1620 Talwani, M. and Eldholm, O.: Evolution of the Norwegian-Greenland Sea.  
1621 *Geological Society of America Bulletin*, 88, 969-999, 1977.
- 1622  
1623 Tchalenko, J. S.: Similarities between shear zones of different magnitudes.  
1624 *Geological Society of America Bulletin*, 81, 1625-1640, 1970.
- 1625  
1626 Tron, V. and Brun, J.-P.: Experiments on oblique rifting in brittle-ductile systems.  
*Tectonophysics*, 188(1/2), 71-84, 1991.
- 1627  
1628 Tsikalas, F., Faleide, J. I., Eldholm, O., and Blaiçh, O. A.: The NE Atlantic conjugate  
1629 Margins. In: Roberts, D.G. & Bally, A.W., *Phanerozoic Passive Margins, Cratonic*  
1630 *Basins and Global Tectonic Maps*, Elsevier, DOI: 10.1016/B978-0-444-56357-  
1631 6.00004-4, 2012.
- 1632  
1633 Twiss, R. J. and Moores, E. M.: *Structural Geology*, 2nd Edition, W.H.Freeman & Co.,  
1634 New York, 736pp, 2007.
- 1635  
1636 Ueta, K., Tani, K. and Kato, T.: Computerized X-ray tomography analysis of three-  
1637 dimensional fault geometries in basement-induced wrench faulting, *Engineering*  
1638 *Geology*, 56, 197-210, 2000.
- 1639  
1640 Uliana, M. A., Arteaga, M. E., Legarreta, L., Cerdan, J.J. and Peroni, G. O.: Inversion  
1641 structures and hydrocarbon occurrence in Argentina. *in*: Buchanan, J.G. &  
1642 Buchanan, P.G. (eds.): *Basin Inversion*, Geological Society London Special  
1643 Publication, 88, 211-233, 1995.
- 1644  
1645 Vågnes, E.: Uplift at thermo-mechanically coupled ocean-continent transforms:  
1646 modeled at the Senja Fracture Zone, southwestern Barents Sea. *Geo-Marine*  
*Letters*, 17, 100-109, 1997.
- 1647  
1648 Vågnes, E., Gabrielsen, R. H., and Haremo, P.: Late Cretaceous-Cenozoic intraplate  
1649 contractional deformation at the Norwegian continental shelf: timing, magnitude  
and regional implications. *Tectonophysics*, 300, 29-46, 1998.

1650 Weijermars, R. and Schmeling, H.: Scaling of Newtonian and non-Newtonian fluid  
1651 dynamics without inertia for quantitative modelling of rock flow due to gravity  
1652 (including the concept of rheological similarity. *Physics of the Earth and Planetary*  
1653 *Interiors*, 43, 316–330, 1986.

1654 Wilcox, R. E., Harding, T. P., and Selly, D. R.: Basic wrench tectonics. *American*  
1655 *Association of Petroleum Geologists Bulletin*, 57, 74-69, 1973.

1656  
1657 Williams, G. D., Powell, C. M., and Cooper, M. A.: Geometry and kinematics of  
1658 inversion tectonics. in: M.A.Cooper & G.D.Williams (eds.): *Inversion Tectonics*.  
1659 *Geological Society of London Special Publication*, 44, 3-16, 1989.

1660  
1661 Willingshofer, E., Sokoutis, D., and Burg, J.- P.: Lithosphere-scale analogue modelling  
1662 of collision zones with a pre-existing weak zone, *in*: Gapais,D., Brun.,J.P.&  
1663 Cobbold,P.R. (eds.): *Deformation Mechanisms, Rheology and Tectonics: from*  
1664 *Minerals to the Lithosphere*, *Geological Society London Special Publication*,43,  
1665 277-294, 2005.

1666  
1667 Willingshofer, E., Sokoutis, D., Beekman, Schönebeck, F., Warsitzka, J.-M., Michael,  
1668 M., and Rosenau, M.: Ring shear test data of feldspar sand and quartz sand used in  
1669 the Tectonic Laboratory (TecLab) at Utrecht University for experimental Earth  
1670 Science applications. V. 1. GFZ Data Service.  
1671 <https://doi.org/10.5880/figeo.2018.072>, 2018.

1672  
1673 Woodcock, N. H. and Fisher, M.: Strike-slip duplexes. *Journal of Structural Geology*,  
1674 8(7), 725-735, 1986.

1675  
1676 Woodcock, N. H. and Schubert, C.: Continental strike-slip tectonics. in: P.L.Hancock  
1677 (ed.): *Continental Deformation* (Pergamon Press), 251-263, 1994.

1678  
1679 Yamada, Y. and McClay, K. R.: Analog modeling of inversion thrust structures,  
1680 experiments of 3D inversion structures above listric fault systems, in: McClay,K.R.  
1681 (ed.): *Thrust Tectonics and Petroleum Systems*, *American Association of*  
1682 *Petroleum Geologists Memoir*, 82, 276-302, 2004.

1683  
1684